N 69 39403
NASA CR-66824

PHOTOGRAPHIC STUDY OF SOLID PROPELLANTS BURNING IN AN ACCELERATION ENVIRONMENT

By P. G. Willoughby, K. L. Baker,
and R. W. Hermsen

Prepared under Contract No. NAS1-8796 by
United Technology Center
Division of United Aircraft Corporation
Sunnyvale, California

for

NATIONAL AERONAUTICS AND SPACE ADMINISTRATION

ACKNOWLEDGMENTS

The idea of photographing propellant burning under acceleration first arose at UTC when the pioneering photographic work on stationary propellants by J. E. Crump and J. D. Hightower at the Naval Ordnance Test Station, China Lake, California, (now the Naval Weapons Center) became known. UTC developed the apparatus under the sponsorship of the Naval Ordnance Systems Command, Contract N00017-67-C-2429, "Investigation of Internal Ballistics Effects in Spinning Solid Propellant Motors." In this work the freely given advice of Messrs. Crump and Hightower was of the greatest value, particularly in respect to the design of the combustion bomb.

During the photographic work and study, fruitful discussions were held by the authors with Dr. C. T. Crowe, formerly senior staff scientist at UTC, now professor at Washington State University, and with G. B. Northam of NASA Langley Research Center. Mr. Northam was carrying out experiments in the field of combustion under acceleration concurrent with the experiments presented in this report; the interchange of data and interpretations was of great benefit to the authors and is sincerely acknowledged.

The excellent clarity and detail of the films is in large part due to the efforts of D. E. Girroir, UTC photographer, who was responsible for film selection and handling, camera exposure and operation, and film processing.

ABSTRACT

The effect of acceleration on the combustion of aluminized composite solid propellants was studied using high-speed color cinematography. Strands of six different propellants were photographed while burning at pressures of 200, 500, and 1,000 psi and at accelerations up to 100 g in a direction normal to and into the burning surface. Strands of one formulation were photographed with the acceleration vector oriented at 75^{o} with respect to the burning surface.

The films showed that aluminum agglomerates, which are known to form on the burning propellant surface under static conditions, were held on the surface in the presence of acceleration forces and coalesced into burning globules. The presence of these globules resulted in the formation of pits in the propellant surface. As burning proceeded the pits coalesced, becoming broader and shallower, and the globules flattened out until they covered almost the entire strand surface. This process is described in terms of a five-stage combustion model.

All of the aluminized propellants studied exhibited the same general behavior; however, the time required for the transition of the globules and pits through the various stages depended on the propellant formulation and on the pressure and acceleration level. Size distributions of aluminum agglomerates on the burning surface were measured from the films for four of the propellants burning at various pressures and accelerations.

An edited motion picture film, consisting of selected film clips from each experiment, is described. Photographs of residual slag and extinguished propellant surfaces taken with a scanning electron microscope are presented and discussed.

CONTENTS

ILLUSTRATIONS

ILLUSTRATIONS (Continued)

TABLES

ABBREVIATIONS

Al	aluminum
Al/Al_2O_3	aluminum/aluminum oxide
AP	ammonium perchlorate
BFG	B.F. Goodrich
$BKNO_3$	boron potassium nitrate
CTPB	carboxy-terminated polybutadiene
DB	distance burned
D_m	mass median diameter
D_n	number median diameter
IR	infrared
M	magnification
Mg/Al	magnesium/aluminum alloy
PBAA	polybutadiene-acrylic acid
PBAN	polybutadiene-acrylic acid-acrylonitrile
P_c	chamber pressure
P_{c_ω}	chamber pressure with spin
NASA	National Aeronautics and Space Administration
$\dot{r}$	burning rate
$\dot{r}_\omega/\dot{r}_\omega$	average burning rate augmentation factor
UTC	United Technology Center
α	radial acceleration

PHOTOGRAPHIC STUDY OF SOLID PROPELLANTS BURNING IN AN ACCELERATION ENVIRONMENT

By P. G. Willoughby, K. L. Baker,
and R. W. Hermsen

SUMMARY

Previous studies have shown that acceleration forces may substantially increase the burning rate of aluminized composite solid propellants by retaining burning aluminum agglomerates on the propellant surface. This report contains detailed observations, made by high-speed color cinematography, of the effect of acceleration on the aluminum agglomeration and combustion processes occurring on the propellant surface. Six different composite propellants were photographed while burning at pressures of 200, 500, and 1,000 psia and at accelerations up to 100 g in a direction normal (90^{o}) to and into the burning surface. Additional photographs were taken of one propellant with the acceleration vector oriented at 75^{o} with respect to the burning surface.

The films show that aluminum agglomerates, which also formed on the burning surface under static conditions but which were quickly entrained by the combustion gases, were held on the surface and coalesced into burning globules when the acceleration forces were present. The retention of these globules resulted in the formation of pits in the propellant surface because of the increase in burning rate near the globule. The globules increased in size by collecting aluminum agglomerates emerging from the pit walls. The pits continued to grow due to increased heat transfer to the propellant surface beneath the burning globules. When the pits covered a large part of the surface, they began to merge forming broader and shallower pits in which the globules coalesced, creating still larger globules which flattened out in the acceleration field. As combustion proceeded, the pits continued to merge and the globules became flatter, until they covered almost the entire surface. The observed history of pit growth, which is described in terms of a five-stage combustion model, correlates well with burning rate transients under acceleration observed by UTC and other investigators.

All aluminized propellants studied exhibited the same mechanism of pit formation and growth. However, the time required for the transition of the pits through the various stages of their development depended on the propellant formulation and on pressure and acceleration level. A high burning rate propellant containing a magnesium/aluminum alloy did not exhibit any acceleration sensitivity.

Size distributions of the aluminum agglomerates on the burning surface were measured from individual frames of the films showing four of the propellants burning at various pressures and accelerations. The mass median diameters of these agglomerates at zero acceleration were widely different for the different propellants, ranging from 130μ to 440μ. The agglomerate size appeared to increase with acceleration and with decreasing pressure level. It was noted that the propellants which formed the larger agglomerates had exhibited greater sensitivity to acceleration in previous experiments.

An edited film consisting of a short documentary on the apparatus and selected film clips from each of the experiments was prepared. This film is available on loan from NASA Langley Research Center (see request form at the end of this report).

Samples of residual slag and extinguished propellant surfaces were studied using photographs taken with a scanning electron microscope. The surfaces of the slag particles contain large numbers of small holes, and the interior structure is characterized by tubular voids. The appearance of the ammonium perchlorate particles in photomicrographs of the extinguished propellant suggests the subsurface evolution of gas and the existence of a liquid layer during combustion.

1.0 INTRODUCTION

Experience has shown that the burning rate of an aluminized solid propellant may be significantly increased in a spinning rocket, that is, in the presence of an acceleration field directed toward the burning surface. Previous studies have indicated that this increase in burning rate probably results from increased heat transfer to the propellant beneath burning aluminum globules that are held on the surface by the acceleration forces. The validity of this mechanism was supported by postfire observation of the surface of grains that had been quenched while burning under acceleration, and by qualitative agreement between theoretical ballistics predictions based upon this mechanism and trends in the experimental data on the relation between burning rate and acceleration. In order to obtain more direct insight into the mechanism of burning rate augmentation, an apparatus for obtaining high-speed motion pictures of a propellant surface burning under acceleration was developed at UTC under sponsorship of the Naval Ordnance Systems Command. Films obtained using this apparatus substantiated the proposed mechanism and, in addition, revealed interesting details of the agglomeration, ignition, and combustion of aluminum on the propellant surface. A review of the previous experimental and theoretical work is presented in section 2.0.

This report presents the results of further studies conducted at UTC under the sponsorship of the NASA Langley Research Center in which high-speed motion pictures were obtained of six different aluminized composite propellants burning at pressures from 200 to 1,000 psi and at accelerations up to 100 g normal to (90^{o}) and into the burning surface. Additional photographs were taken of a single formulation with the acceleration vector oriented at 75^{o} with respect to the burning surface. The experimental apparatus used was the same as that developed for the previous studies and is described in section 3.0. The resulting films show the coalescence and ignition of aluminum and further agglomeration to form large globules on the propellant surface. These burning globules form pits in the propellant surface which change in shape and size as burning progresses. Observations made during the formation, growth, and changing shape of these globules and pits, along with observations made during recent studies at NASA Langley Research Center, provide a complete qualitative explanation of the variations of the burning rate under acceleration. These observations are discussed in detail in section 4.0. The size distributions of Al/Al_2O_3 agglomerates on the propellant surface were determined from several film frames and are discussed in section 4.0; scanning electron photomicrographs, which show Al/Al_2O_3 residues collected from the combustion bomb, have been included.

The most illustrative portions of the films taken during each experiment were made into a single composite film using subtitles and including a short documentary on the apparatus. This film is described in section 5.0.

2.0 REVIEW OF PREVIOUS EXPERIMENTS AND THEORETICAL MODELS

The important influence of an acceleration field on the performance of solid propellant propulsion systems became evident during the early development of spin-stabilized vehicles. Increased thrust and decreased burning time, together with increased metal oxide slag retention and increased local heat transfer, were experienced in development firings of small rocket-assisted projectiles as well as spin-stabilized upper-stage motors.[1]*

Once it had been observed that acceleration influences the combustion of solid propellants, experiments were conducted to obtain quantitative data for conventional aluminized and nonaluminized composite propellants with burning rates ranging from 0.15 to 1.0 in./sec.[2 through 8] A review of this work has been presented earlier,[2] and the conclusions are summarized in the following paragraphs.

During all experiments in which the acceleration vector was perpendicular to and directed toward the burning surface (as in a spinning, cylindrical internal burning grain), an increase in burning rate was observed. In experiments performed with the acceleration vector oriented parallel to the burning surface, there was no discernible change in burning rate.[6,8] Studies in which Northam and Lucy varied the angle between the acceleration vector and the burning surface showed that, in the acceleration regime of their experiments, the propellant burning rate was substantially equal to the static value whenever the angle was less than 75°.[5] Other experiments have demonstrated that the burning rate was not appreciably changed from its static value when the acceleration vector was directed away from the burning surface.

The experimental evidence indicates further that for most propellants the burning rate changed very little until a threshold acceleration level was reached and then became very sensitive. As the acceleration level was increased further, it was observed that the burning rate tended to approach an asymptotic value.

The burning rate exhibited a transient behavior during tests in which the acceleration level at the burning surface remained relatively constant. During experiments at UTC[2] using internally burning subscale motors with 0.6-in. propellant webs spun about their centerlines, the burning rate started at a value higher than under static conditions and then increased steadily with time under most conditions. However, at high chamber pressures or high acceleration levels, the burning rate reached a maximum and then decreased with time. This transient behavior has recently been investigated in detail by Northam using the Langley Research Center slab burner.[9]

In addition to verifying the results discussed above under conditions of more closely controlled constant acceleration, Northam's data show an interesting correlation between the shape of pits that form in the burning surface, the nature of slag residue, the instantaneous burning rate, and the thickness of web burned. This correlation is illustrated in figure 1, which is a composite of two figures from reference 9. As burning progressed, the burning rate first increased while the slag remained largely spherical and the pits in the propellant surface increased in diameter. After the maximum in burning rate augmentation was reached, the pits continued to increase in diameter and the burning rate decreased to approach a constant value, while the slag changed progressively from spheres to buttons to irregular puddles, and finally, into a continuous sheet. These results, together with the photographic studies discussed in this report, provide a reasonably complete picture of the observed burning-rate transients, as presented in section 4.0.

---

* Parenthetical superscript numbers denote references appearing on page 54.

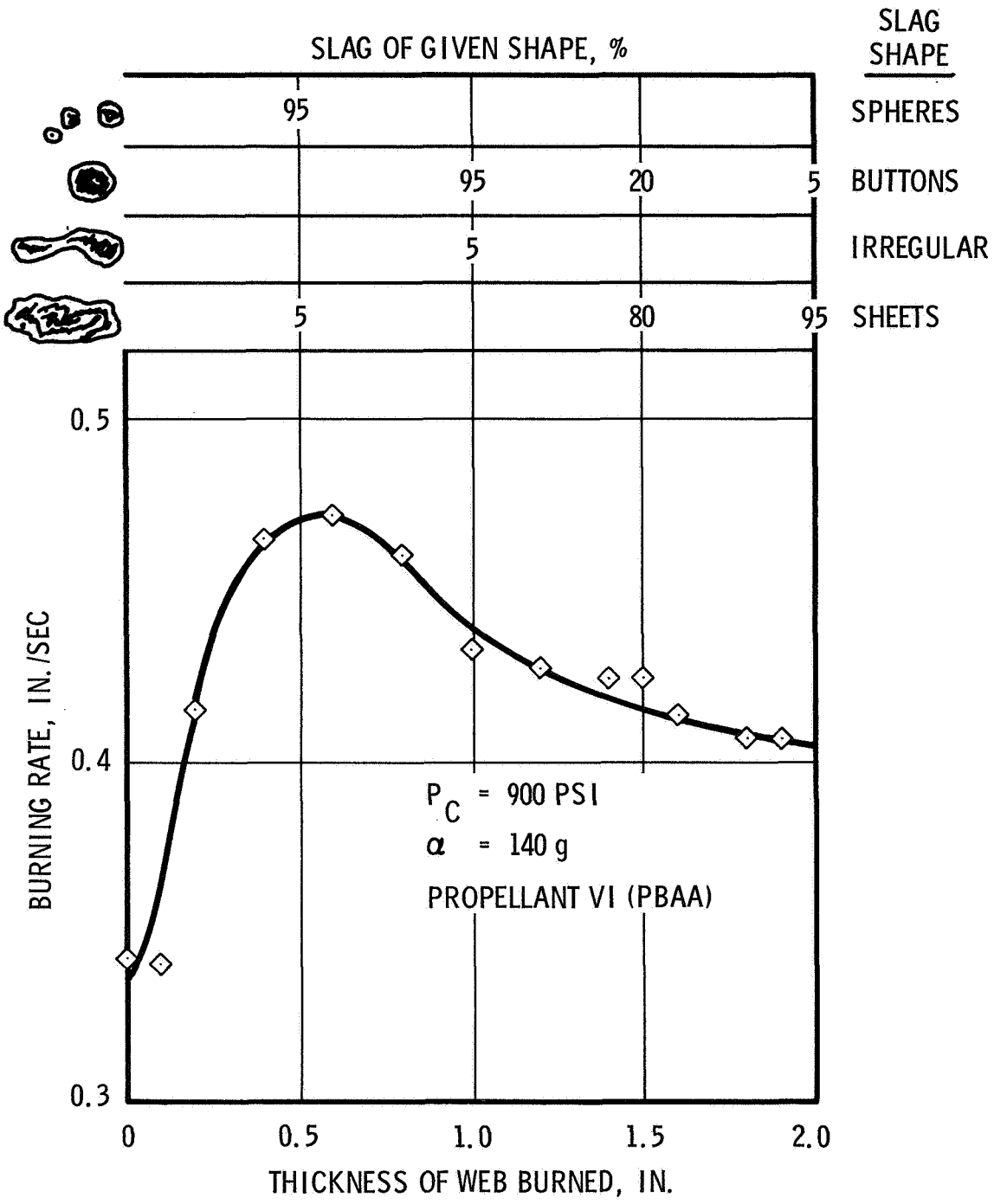

Figure 1. Correlation Between Slag Shape and Spin-Augmented Burning Time

91486

Another major parameter which influences the acceleration sensitivity of the propellant was found to be the static burning rate, that is, the burning rate in the absence of acceleration. Because the static burning rate is dependent on propellant formulation and chamber pressure, it is difficult to separate the effects of these variables. However, experiments conducted at UTC using two propellant formulations, each with and without a burning-rate catalyst, clearly indicate that the burning rate dependency on acceleration level is less for propellants with high static burning rates. For example, one propellant formulation with a static burning rate of 0.25 in./sec at 500 psi approximately doubled in burning rate under 575-g acceleration. The same formulation with 3% of the binder replaced by a burning-rate catalyst had a static burning rate of 1.03 in./sec at 500 psi, and this rate was not measurably different at the high acceleration level.

The effect of the propellant formulation variables, aluminum loading and particle size, ammonium perchlorate particle size, and binder type have also been studied. These variables affect the acceleration sensitivity of the propellant through changes in the static burning rate. The formulation variables also influence the size of the aluminum agglomerates which form on the burning propellant surface. As will be discussed, these agglomerates play an important role in the mechanism by which acceleration increases the burning rate.

Photographic studies of composite propellants burning under static conditions have shown that the aluminum particles contained in the propellant coalesce to form particles 100μ to 300μ in diameter.[10] These particles usually move about and ignite before leaving the propellant surface. It has been postulated[4] that acceleration holds these coalesced particles on the surface and that the increase in heat transfer to the surface, resulting from retention of the particles, is responsible for the increased burning rate. The burning-rate augmentation in the initial model was assumed to be uniform over the burning surface.

Further information was gained by Northam, who observed the surface of propellant grains extinguished while burning under acceleration.[6] The grains were severely pitted, and globules of Al/Al_2O_3 slag were found in some of the pits, suggesting that the coalesced particles agglomerate, form pits, and are retained on the surface until propellant burnout.

Based upon this information, Glick extended the original UTC model to account for pit formation.[13] A more detailed model was subsequently formulated by UTC in which the increase in burning rate is caused by an increase in heat transfer beneath burning globules held in the bottom of the pits by acceleration forces.[2,11] This model is illustrated in figure 2. Gases evolving from the propellant surface must flow out from beneath the globule; therefore, a higher pressure must exist on its underside which buoys the globule against the acceleration forces. The balance between the acceleration and the buoying forces establishes the separation distance between the globule and the surface which, in turn, determines the heat transfer rate from the hot globule to the surface.* If it is assumed that the globule shape in the acceleration force field can be represented by an oblate spheriod, the resulting expression for burning-rate augmentation is

* Aerodynamic forces on the globule resulting from skin friction are small compared to the pressure forces and were not included in the study.

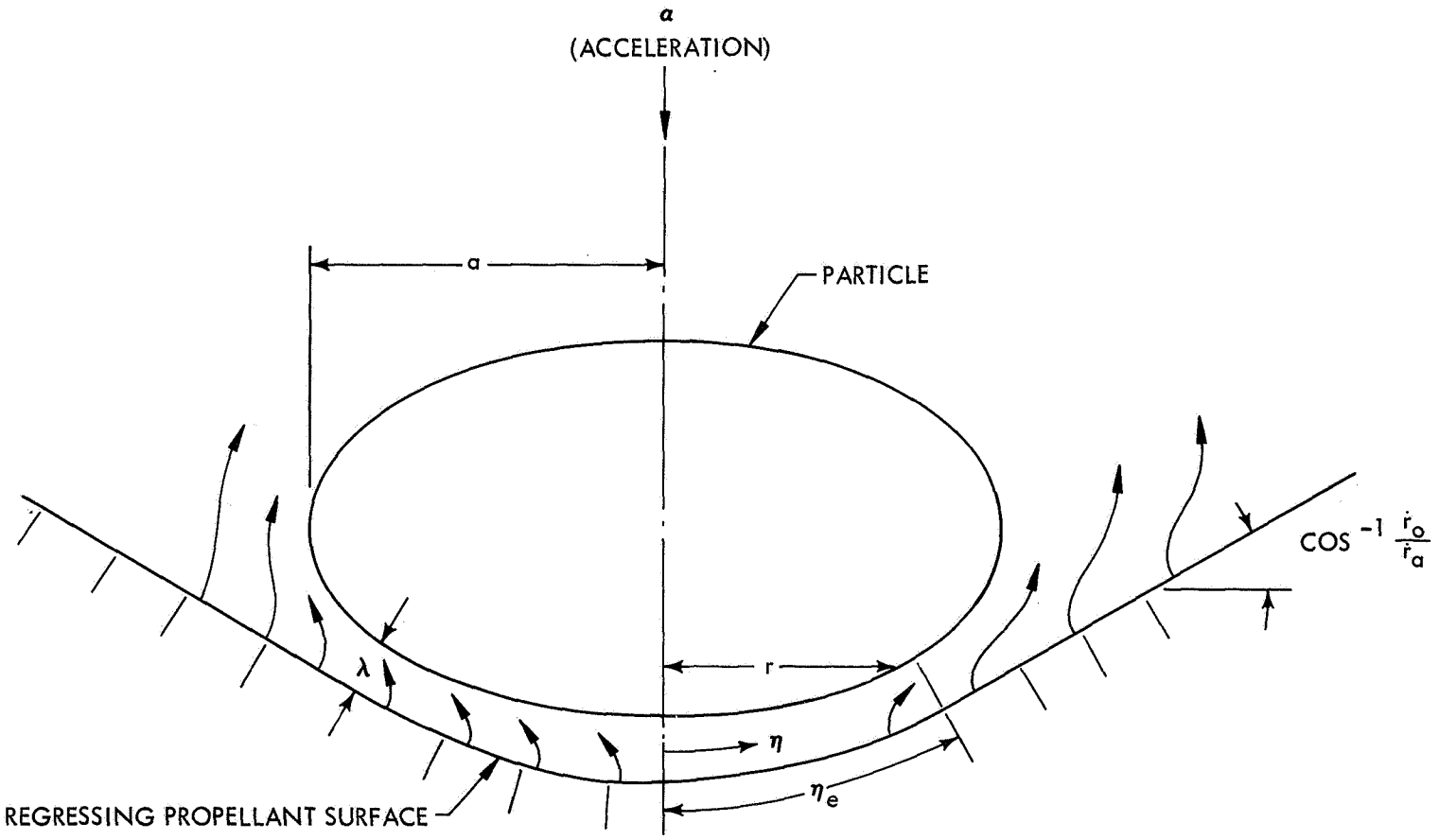

Figure 2. Proposed Physical Model

91487

$$\frac{r_s}{a}\left(\frac{\rho_p P_c \alpha}{r_s}\right)^{1/4} \frac{1}{\rho_s \dot{r}_o (1-w)} = F\left(\frac{\dot{r}_a}{\dot{r}_o}, e\right)$$

where:

r_s = equivalent sphere radius

a = maximum dimension of the globule

ρ_p = globule density

P_c = chamber pressure

ρ_s = propellant density

α = acceleration level

$\dot{r}_o$ = static burning rate

w = weight fraction of metal in the propellant

The term r_s/a accounts for the eccentricity of the globule and is equal to 1 for a sphere. The function $F(\dot{r}_a/\dot{r}_o, e)$ increases monotonically with the burning-rate augmentation ratio, $\dot{r}_a/\dot{r}_o$, and is only slightly dependent upon the globule's eccentricity, e (see figure 6 of reference 2).

This equation predicts several of the observed trends, such as the increased burning-rate augmentation experienced with slow-burning propellants and at high acceleration levels. The model also predicts decreasing augmentation with increasing globule size. The equation further agrees qualitatively with the observed pressure dependence of the burning-rate augmentation of polyurethane propellants. It does not, however, account for the transient effect discussed previously, where r_s and a are functions of time.

Further support for the proposed model was provided by high-speed photographic studies of a composite propellant burning in an acceleration field.[11] The films clearly showed the retention of burning globules on the propellant surface, the persistence of pits formed by the globules, the travel of burning coalesced aluminum along inclined surfaces, and the collision and agglomeration of the coalesced particles.

Current knowledge of the basic composite propellant combustion processes is quite inadequate as a basis for assessing the effects of acceleration; therefore, the photographic studies proved to be of great value in determining the detailed changes in propellant surface combustion phenomena caused by an acceleration field, and in providing data required for predicting slag accumulation. The photographic studies were extended to include higher accelerations and several different propellant formulations on which data were available from previous spinning motor or slab burner experiments. The purpose was again to provide insight into the propellant combustion characteristics which lead to the observed burning rate and slag retention behavior.

3.0 EXPERIMENTAL APPARATUS AND PROPELLANT INFORMATION

3.1 EXPERIMENTAL APPARATUS

The apparatus used for photographing the surface of a burning solid propellant under acceleration normal to the burning surface is shown in figures 3 and 4. The apparatus comprised three main components: centrifuge, combustion bomb, and optical system.

3.1.1 Centrifuge

The centrifuge consisted of a 24-in.-diameter, 0.5-in.-thick aluminum table driven by a 1-hp electric motor through a variable speed hydraulic transmission. The table was capable of rotating at a maximum rate of 1,800 rpm producing an acceleration of 900 g at a radius of 9.75 in. where the burning surface was located. The centrifuge was equipped with an electrical slip ring assembly with four pairs of 5-amp leads and four pairs of 0.5-amp leads which terminated at binding posts on the periphery of the table. This assembly was used to transmit power to the photographic light source and shutter, to the propellant igniter, and to the purge solenoid valve.

Four high-pressure lecture bottles, a pressure regulator, and a solenoid valve were mounted on the table to provide purge gas to the combustion bomb. Time delay relays were used to properly sequence the light source, purge gas valve, camera, and igniter.

3.1.2 Combustion Bomb

The combustion bomb, similar to the combustion bombs used by investigators at the Naval Weapons Center, is shown in figure 5. Three Plexiglas windows were located around the circumference of the bomb at 0^{o}, 30^{o}, and 180^{o}. The windows at 0^{o} and 180^{o} were used for photographic observation, and the window at 30^{o} was used for illumination. The square propellant samples had 0.25- to 0.30-in. sides and were 0.20 to 1.50 in. long. They were mounted in the center of the bomb on a square rod with 0.25-in. sides. On the two sides away from the camera, the samples were inhibited with methylmethacrylate applied in a chloroform solution. Nitrogen flowed continuously and uniformly past the sample at 2 ft/sec to prevent the accumulation of smoke in the optical path during propellant burning. The propellant was ignited with a 0.010-in.-diameter hot wire in conjunction with nitrocellulose glue and $BKNO_3$ powder.

The combustion bomb was connected by 3/8-in. stainless steel tubing to a tank of similar size and weight located radially opposite the bomb on the centrifuge table. The tank served as both pressure ballast and counterbalance; it contained a blowout disc to prepressurize the system and an orifice to regulate the velocity of the nitrogen flowing past the propellant sample. A transducer mounted on the combustion bomb was used to measure the combustion pressure.

3.1.3 Optical System

One corner of the propellant strand was viewed at an angle of 13^{o} to the burning surface with the camera focused approximately 0.15 in. above the mounting post and 0.12 in. in from the front corner as

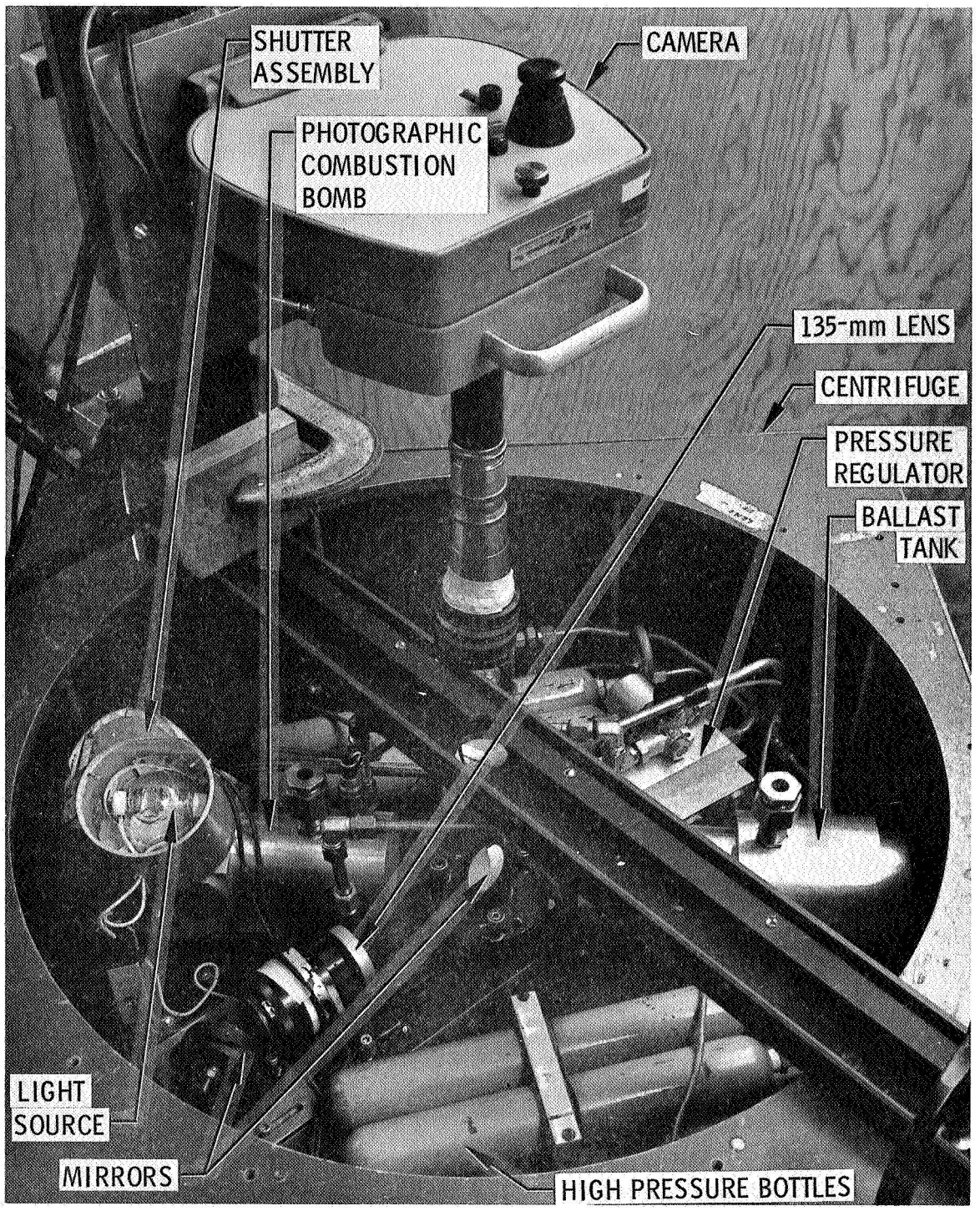

Figure 3. Experimental Apparatus for Photographic Combustion Studies

91505

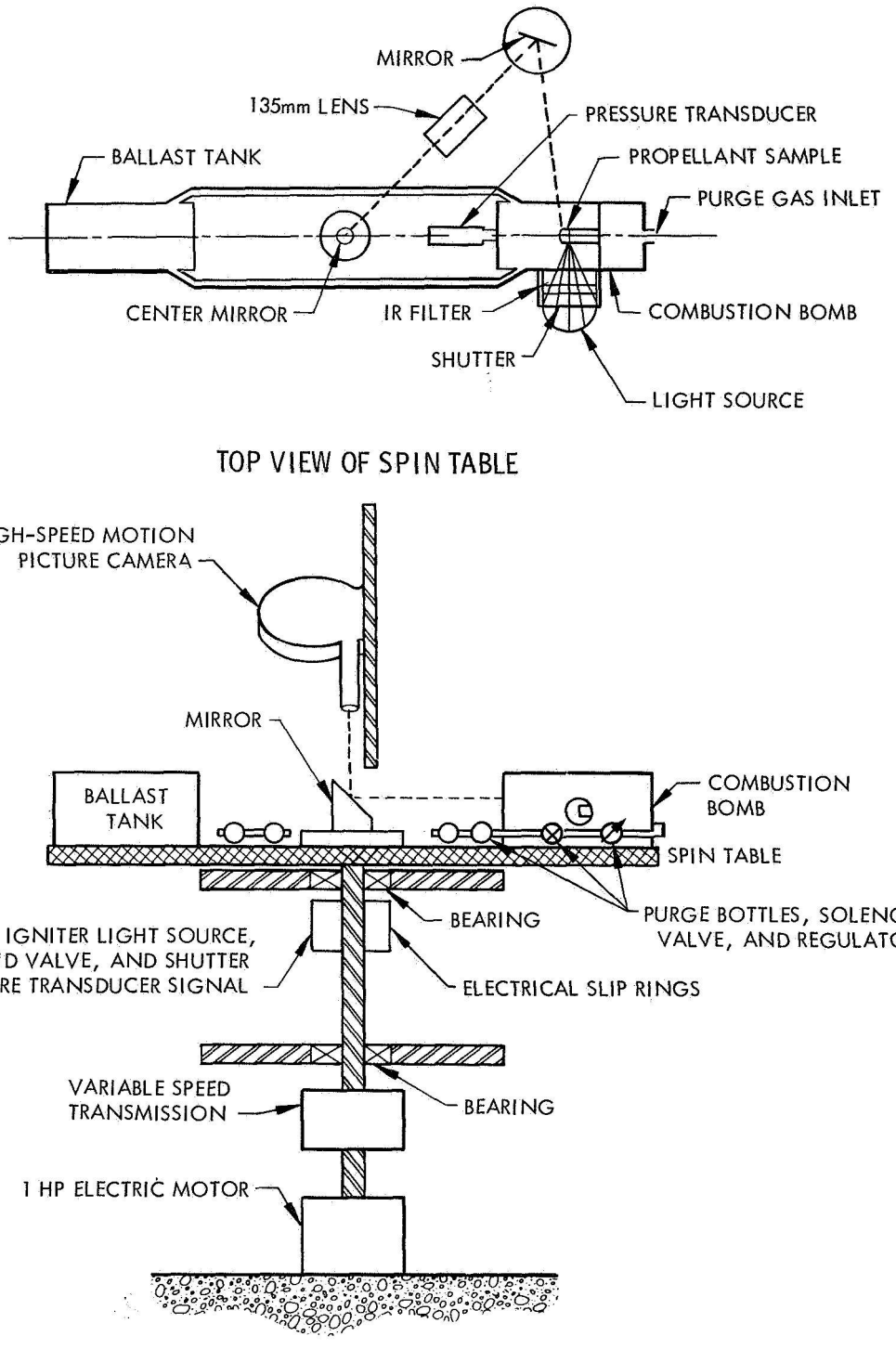

Figure 4. Schematic Diagram of Experimental Apparatus for Photographic Combustion Studies

91488

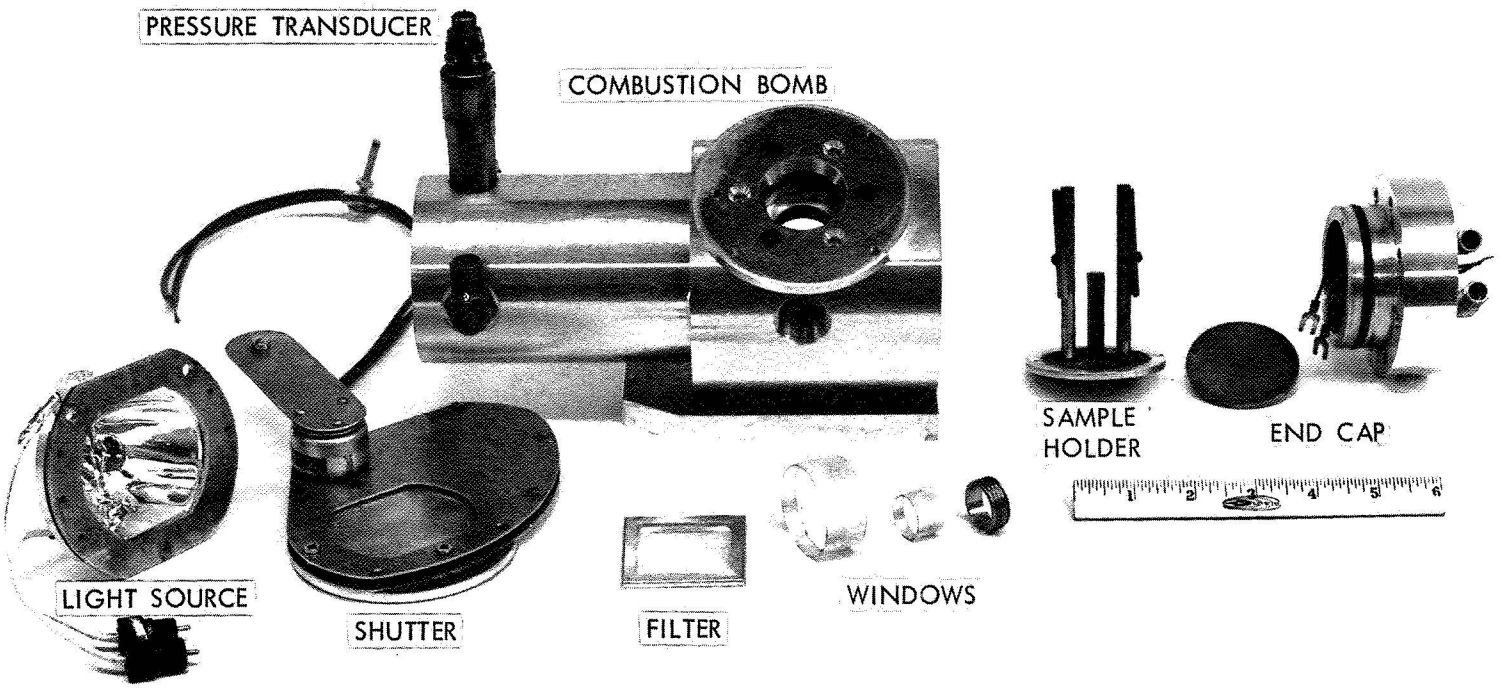

Figure 5. Exploded View of Combustion Bomb for Photographic Combustion Studies

91489

shown in figure 6. The image of the burning propellant sample was projected through a 135-mm Nikkor-Q Auto 1:3.5 lens and a mirror system on to the stationary camera mounted above the table, as illustrated in figures 3 and 4. Using this arrangement, the projected image rotated with respect to the camera. When the films are projected, the combustion sequence can still be observed quite well because the rotation rate of the image is slow when the high-speed film is projected at normal frame speed. This rotation will not create any handicap in data analysis if each frame is examined separately.

Illumination was supplied by a General Electric Marc 300/16 arc lamp mounted in a dichroic reflector. A hot-mirror IR interference filter was inserted between the light source and the propellant sample to restrict the incident radiation to the usable visible light. A radiant flux of 2 to 3 cal/cm^2/sec was measured using a calorimeter placed at the position of the propellant surface in the test section. The hot-mirror IR interference filter cracked during some of the first tests, but it continued to reflect the IR radiation and operated satisfactorily during the remainder of the program. In some cases the light from the burning aluminum particles was the only illumination used.

Two different high-speed motion picture cameras were used during the program. The majority of the films were obtained using a standard 16-mm Hycam 100-ft model camera built by Red Lake Laboratories. This camera has a speed range of up to 9,000 full frames/sec. Several films were made using a Hycam 400-ft model with a speed range of up to 11,000 frames/sec full frame and 22,000 frames/sec using a half-frame optical head. Films taken with the half-frame head were not satisfactory because the rotating image of the burning propellant sample did not continuously remain within the narrow frame width.

The color film used was Kodak EF Daylight Film, ASA 160, which is especially designed for high-speed photographic work. The camera aperture was generally set at f/4.5. The film exposure was controlled by changing the aperture of the lens on the rotating table. A typical exposure for propellant III at 200-psig pressure was made using a lens aperture of f/16, a shutter speed of 1/18,000 sec, and a frame rate of 6,000/sec. It became evident that adequate self-illumination from the burning particles was available for framing rates much higher than those attempted in this study. It was necessary to reduce the aperture of the system when observing a propellant at higher pressures because the gas density and, consequently, the number density of the burning particles was higher and provided greater illumination at the burning surface.

The desired magnification of the image on the film was obtained using a combination of auxiliary lenses and extension tubes attached to the camera objective lens. The magnification and test conditions for each experiment are given in table IV (see section 5.0).

3.2 PROPELLANT FORMULATION AND BALLISTIC DATA

The propellant formulations and their nominal mass median ingredient sizes and ballistic properties are given in table I. Propellants I, II, and III were PBAN formulations. Propellant I was characterized by large ammonium perchlorate and aluminum particle size and served as a control. Propellants II and III were formulated to study the effect of reducing the size of the ammonium perchlorate and aluminum particles upon the spin sensitivity of the propellant. Propellant IV was a low burning rate polyurethane formulation, and propellant V was a moderate burning rate CTPB formulation containing a magnesium/aluminum alloy fuel. Propellant VI was the PBAA formulation studied by Northam.[5,6,9]

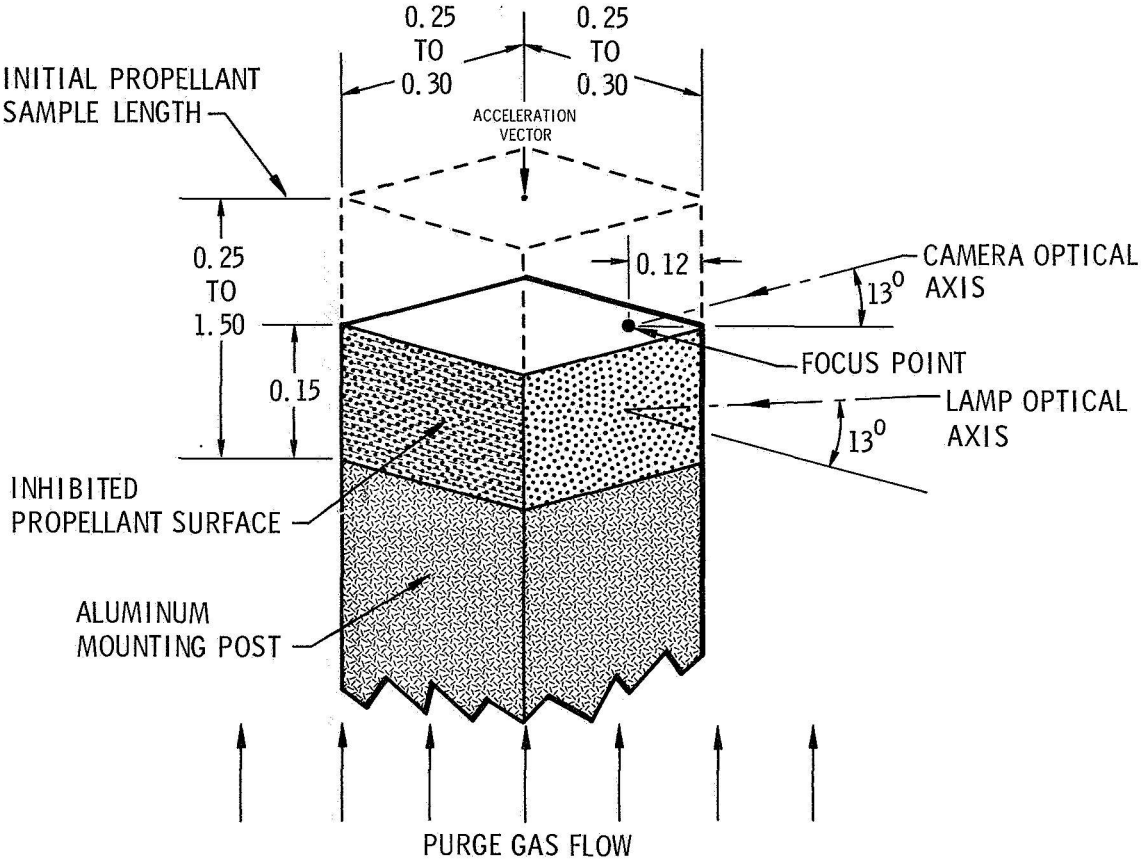

NOTE: ALL DIMENSIONS SHOWN IN INCHES

Figure 6. Schematic Diagram of Sample Orientation and Camera Viewing Angle

91490

TABLE I

PROPELLANT FORMULATION AND BALLISTIC DATA

	Propellant I	Propellant II	Propellant III
Binder	16% PBAN	16% PBAN	16% PBAN
Oxidizer	68% AP 65% 400μ, 35% 8μ	68% AP 40% 190μ, 60% 8μ	68% AP 65% 400μ, 35% 8μ
Metal Fuel	16% Al 46μ	16% Al 46μ	16% Al 8μ
Ballistic Data	$\dot{r} = 0.25\left[\frac{P_c}{1{,}000}\right]^{0.21}$	$\dot{r} = 0.35\left[\frac{P_c}{1{,}000}\right]^{0.20}$	$\dot{r} = 0.34\left[\frac{P_c}{1{,}000}\right]^{0.28}$

	Propellant IV	Propellant V	Propellant VI
Binder	25% Polyurethane	16% CTPB	14% PBAA
Oxidizer	57% AP 200μ	68% AP 70% 200μ, 30% 20μ	70% AP 70% 190μ, 30% 20μ
Metal Fuel	18% Al 26μ	16% Mg/Al Alloy	16% Al 7μ
Ballistic Data	$\dot{r} = 0.13\left[\frac{P_c}{1{,}000}\right]^{0.06}$	$\dot{r} = 0.56\left[\frac{P_c}{1{,}000}\right]^{0.42}$	$\dot{r} = 0.37\left[\frac{P_c}{1{,}000}\right]^{0.25}$

4.0 COMBUSTION UNDER ACCELERATION

High-speed films were made of six composite propellants burning at pressures from 200 to 1,000 psia and accelerations up to 100 g, using the photographic apparatus described in section 3.0. The experimental conditions for each test conducted during this program are listed in table II. These tests significantly extend the previous studies, which were limited to a single propellant burning at 280 psia and to acceleration levels below 50 g.

The results fall somewhat naturally into two groups: (1) a set of observations of aluminum combustion and pit formation and growth which are generally characteristic of all propellants and experimental conditions and (2) specific observations which depict the influence of each of the variables upon propellant combustion. General observations concerning the effect of acceleration on the aluminum combustion process and the formation and growth of pits are discussed in section 4.1, and specific differences between the propellants under various experimental conditions are discussed in section 4.2. In addition to the combustion films, scanning electron micrographs were taken of slag residue, extinguished propellant samples, and aluminum particles, as presented in section 4.3.

4.1 GENERAL OBSERVATIONS

Previous studies have shown that metalized composite propellants are more sensitive to spin than nonmetalized propellants. Furthermore, it was found that reducing the metal powder size and content or using finer oxidizer reduced the acceleration sensitivity of propellants. The principal objective of the experiments was to study in detail the influence of an acceleration field on aluminum combustion near the propellant surface. After viewing films of all the experiments listed in table II, it appeared that the aluminum combustion phenomena could be divided into two main categories: those common to all propellants, pressures, and acceleration levels and those occurring only under acceleration.* The first category includes the combustion of single particles, agglomerates, and sintered masses of particles and has been studied previously at the Naval Weapons Center. The second category is concerned mainly with the formation and growth of pits in the burning propellant surface.

One of the most important phenomenon observed under all conditions was the agglomeration of the small aluminum particles that were cast in the propellant into large particles on the propellant surface. The size of these agglomerates appeared to control the time dependence and magnitude of the spin sensitivity of the propellant. Even though the size of the agglomerates varied for each propellant and operating condition,

* The magnesium/aluminum formulation, propellant V, did not exhibit any sensitivity to acceleration under the test conditions. Therefore, the observations and conclusions in the following discussion do not apply to this propellant.

TABLE II

EXPERIMENTAL CONDITIONS

Propellant	Pressure psia	Acceleration Level g				
		0	25	50	75	100
I	200	1	—	—	—	5*
	500	1	1	1	1	1
	1,000	1	—	—	—	1
II	200	1	—	—	—	4* †
	500	2	1	1	—	1* †
	1,000	1	—	—	—	1
III	200	1	—	—	—	4*
	500	1	1	1	—	1
	1,000	1	—	—	—	1
IV	200	1	—	1	—	—
	500	1	—	1	—	1
	1,000	1	—	1	—	—
V	200	1	—	—	—	1
	500	1	—	1	—	1
	1,000	1	—	—	—	1
VI	200	1	—	—	—	2*

* Runs made at different magnifications and framing rates or with different sample lengths

† Runs in which the acceleration vector was oriented at 75^{o} with respect to the burning surface

in all cases the process appeared to be similar to that shown in figure 7* (figure 7 is composed of frames taken from film No. 36 which shows the polyurethane propellant IV burning at 200 psi under static conditions). In frame 7-1 several aluminum particles emerge from the propellant; in frame 7-2 they have formed a chain and are starting to coalesce; in frame 7-3 the agglomerate is completely formed and has ignited; in frame 7-4 the agglomerate leaves the propellant surface and continues to burn as it moves with the gas stream out of the field of view.

In general, the agglomerates moved about on the surface prior to igniting and leaving. This motion occurred during the agglomeration process and was probably the result of surface forces which drew a chain of particles together, as is easily seen in the movie sequence, but is difficult to detect at higher pressures and burning rates. This phenomenon has been reported by investigators at the Naval Weapons Center, and is important in understanding the influence of acceleration upon propellant combustion, as will be discussed.

This series of frames also provides some insight into the aluminum combustion process. In each of the frames, all the burning aluminum particles have bright tails which are characteristic of vapor phase combustion. In frame 7-4 there is a cap on the large agglomerate, which is presumably aluminum oxide that was formed during the ignition process and may have continued to grow by surface combustion of additional aluminum. The existence of the cap indicates that after the agglomerate burns out there will be an oxide residue which is large with respect to the size of the submicron vapor-phase combustion products. It is also significant with respect to nozzle and aft closure heat transfer in which particle impingement depends critically on size distribution. The effect of formulation variables, pressure, and acceleration on agglomerate size is discussed in section 4.2.

The other two modes of combustion generally observed under all conditions were the burning of single particles and of sintered clusters of particles. Single particle combustion took place when a particle cast in the propellant was ejected from the surface and burned alone. This mode of combustion was characterized by small bright flashes in individual frames. The combustion of sintered groups of particles occurred rather infrequently but did take place under all conditions. This mode of combustion began like the normal agglomeration process, but after ignition and ejection from the surface (see figure 7, frames 7-1, -2, and -3), the sintered agglomerate disintegrated and burned as individual particles. The relative importance of sintered clusters and agglomerates depended on the specific propellant formulation, chamber pressure, and acceleration level.

---

* The photographic prints contained in this report are incapable of conveying the detail and providing the understanding that is available from the original films. This is principally due to the loss of motion; but, in addition, the exposure latitude and color tones of the original film could not be reproduced successfully. Color positive film was used throughout this study; therefore, the photographs presented in this report required that black and white negatives be made from the original film. In an attempt to reproduce the extreme exposure latitudes in the original 16-mm color film, the film used for the black and white negatives was pre-exposed. Each negative was then custom printed. These prints still do not reflect the quality of the original color positives viewed with transmitted light. An alternate approach to obtain quality black and white photographs to aid in presenting the results of similar studies would be to take a limited number of high-speed films using black and white fine-grain negative film. The exposure and processing of these films could be controlled to yield high quality negatives directly.

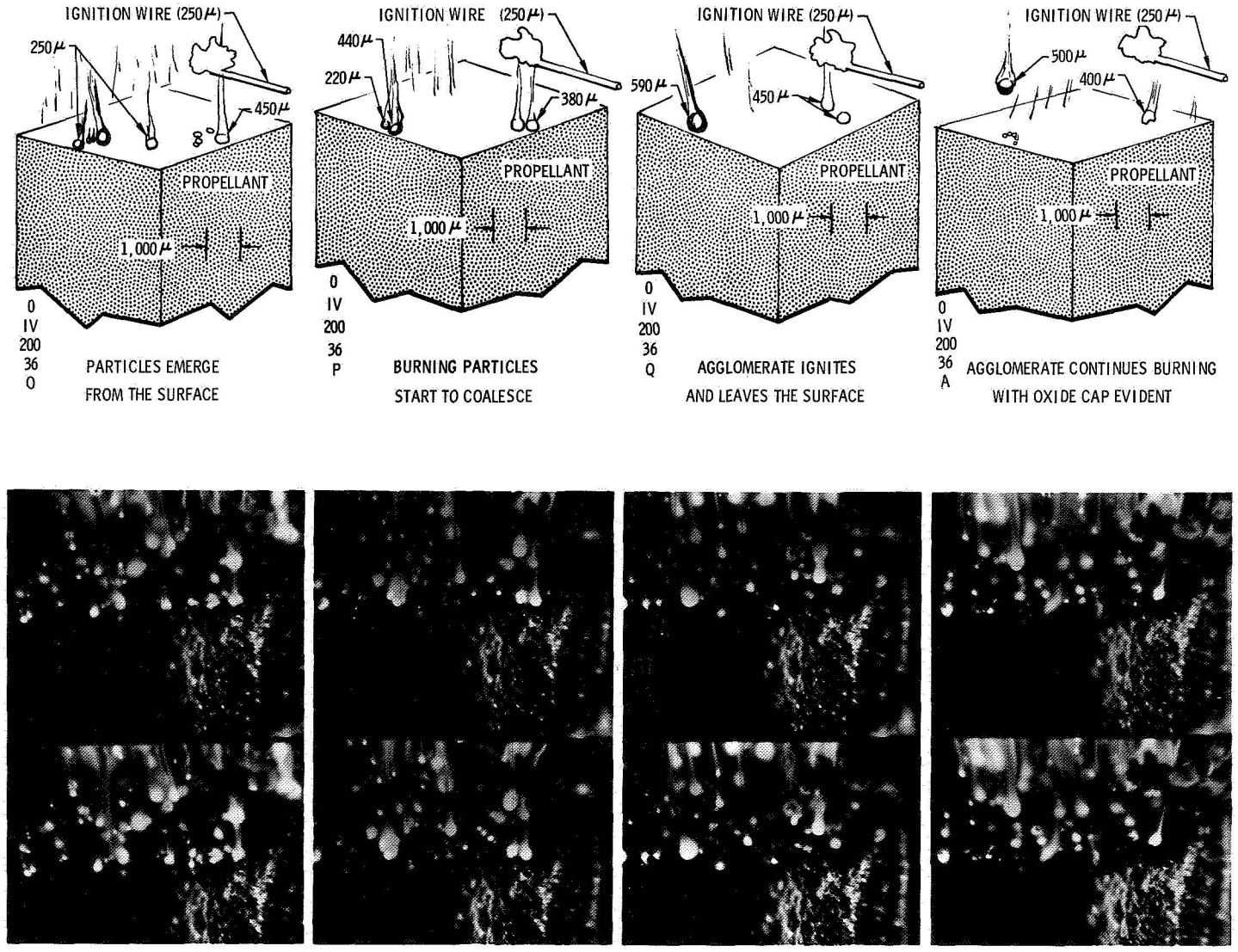

Figure 7. PHOTOGRAPHS AND SCHEMATIC DIAGRAMS OF ALUMINUM AGGLOMERATION ON SURFACE OF POLYURETHANE PROPELLANT (PROPELLANT IV) BURNING AT 200 PSI

91491

The most striking change in combustion resulting from acceleration was the formation of pits in the propellant surface. The initial model for combustion under acceleration assumed that the aluminum agglomerates were retained on the surface by the acceleration field until they had burned to a mass small enough to be carried away by the combustion gases. Inspection of the grains extinguished during firing revealed a severely pitted surface indicating that the retention of agglomerates on the surface had caused the formation of the pits. The films obtained during the present studies showed that these two processes competed immediately following ignition (and probably at later times on level portions of the propellant surface), with pit formation and growth becoming dominant as burning continued.

The process of pit formation and growth shown in the films followed the same general course for all propellants and experimental conditions; however, the time required for development and transition through the various stages was a function of these variables. The five more or less distinct stages in the continuous process are illustrated in the series of schematic diagrams and photographs shown in figure 8.* Stage 1 occurred soon after ignition when a large number of small coalesced aluminum particles had appeared on the burning surface. The particles were held on the surface by acceleration forces, moved about randomly, and as time progressed they combined to form fewer but larger agglomerates, which proceeded to form distinct individual pits resulting in stage 2. During stage 3, as burning continued, the pits merged forming broader shallower pits, and the agglomerates coalesced further into globules so large that surface tension was no longer sufficient to maintain a spherical shape under the acceleration field. Stages 4 and 5 resulted as the puddle continued to grow until finally the entire surface was covered with Al/Al_2O_3 slag. This description of the combustion process under acceleration is consistent with the observations of Northam, who studied the shape of pits and slag on slabs of solid propellant (15-in.^{2} surface area) that had been extinguished after burning for various times under acceleration.[9] The choice of the five stages described above is arbitrary because the entire process of pit formation and growth progressed continuously as the propellant burned.

After ignition, the time to reach stage 1 was the same as that required for individual particles in the propellant to coalesce, as was discussed previously. The number of larger particles which were retained on the surface depended on their size, the propellant formulation, pressure, and acceleration level. During the transition from stage 1 to stage 2 the particles "danced" about the surface, apparently in response to aerodynamic forces exerted by the combustion gases and to interactions with particularly active places on the surface, which appeared to correspond to the location of ammonium perchlorate particles in the propellant surface.

The burning aluminum particles often appeared to avoid one another because of the gas flow field around each particle. In some of the films (e.g., No. 16) these aluminum particles could be observed to form, ignite, and burn down to a considerably smaller diameter (from 500μ to 300μ) at which time they turned dull red and appeared to extinguish. Additional aluminum would then impinge on the particle, which would reignite and then burn down again. Once stage 2 has been reached, the larger spherical agglomerates characteristic of this stage caused deep pits to form; in many cases the pits were so deep that the agglomerate disappeared from the field of view. Once a pit had developed, the large agglomerate was fed

* The photographs from reference 9 showing the extinguished grain surfaces may present an optical illusion to the viewer, as the depressions (pits) appear to be mounds.

by smaller coalesced particles which formed on the pit wall, ignited, and slid down along the wall, colliding with and burning on the main particle in the bottom. When a particle was observed to emerge from the pit wall, it did not appear to be free to move downward until it had ignited. This behavior would occur if the forces which sinter the original particles together were greater than the acceleration forces. Throughout stages 1 and 2 the Al/Al_2O_3 slag particle retained a spherical shape and burned in a stable manner in the bottom of the pit; a few particles would fall off the edge of the burning surface due to the acceleration field.

As burning continued, the pits formed in stage 2 grew together forming broader and shallower pits, and particles in adjacent pits coalesced to form still larger globules, 3,000μ to 4,000μ in diameter. During stage 3 the pits were saucer shaped and the globules were button shaped in the equilibrium position. However, the globules no longer retained a stable shape but began to move violently about in their pits. This motion appeared to result from processes occurring inside the globule as well as from interactions between the globule and the surface. Most of the movement was caused by jets of combustion gases issuing from the propellant surface. Depending on the size and intensity of these jets, the globule was either lifted from the surface, pushed about, or broken up. However, occasionally the globule would fly apart, apparently because of rapid internal combustion reactions. As combustion typical of stage 3 proceeded, the movements of the particle became increasingly violent and caused portions of the Al/Al_2O_3 globule to be thrown off the burning surface. In some instances the pit would break through the edge of the propellant strand and the entire globule would flow off the surface.

The phenomena discussed above are illustrated in figure 9 by selected frames from the films; also shown in the figure are photographs of the surfaces of propellant grains extinguished while burning under acceleration. The conditions under which the extinguished grains were fired are not identical to those under which the selected frames were taken, but their appearance is representative of stages 2 and 3. In frame 1, stage 2 combustion is well established, and a number of pits containing burning spherical Al/Al_2O_3 particles are visible, corresponding to the pits in the extinguished grain surface. Frame 2 shows two large agglomerates that are about to coalesce, which is typical of the transition from stage 2 to stage 3. Frame 3 was taken during combustion and the asymmetric shape of the large globule is evident. In frame 4 a globule similar to that in frame 3 is shown cooling in the characteristic shape of a button. The extinguished grain in frame 3 shows the shallow saucer-shaped pits characteristic of this stage of combustion.

The films of combustion at stage 3 indicate that as time progresses the pits will simply become broader and shallower and the slag globules will continue to grow until they cover almost the entire surface. Stages 4 and 5 could not be studied because the limited burning surface area available with the current apparatus allowed the globules to spill over the sides. The films also indicate that the large Al/Al_2O_3 slag puddles associated with stage 4 and 5 combustion are undoubtedly subject to violent motion under the influence of surface and interparticle phenomena.

The effect of the angle between the acceleration vector and the burning surface was also investigated since Northam had demonstrated it to be an important variable.[6] This was accomplished using the same photographic combustion apparatus by cutting the top of the strand to the desired angle. Samples of propellant II, which contains small ammonium perchlorate, were photographed while burning at 200 and 500 psi under static conditions and at 100 g with an angle of 75° between the acceleration vector and the

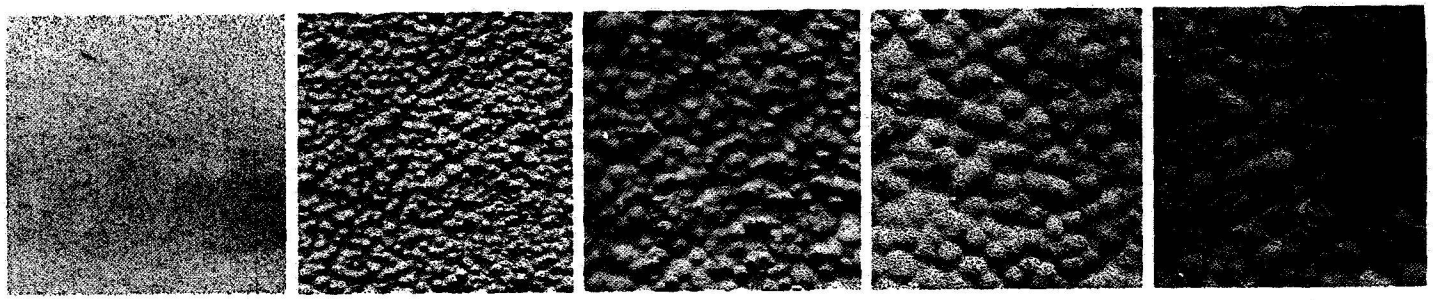

Figure 8. PHOTOGRAPHS AND SCHEMATIC DIAGRAMS OF PIT FORMATION AND GROWTH

91492

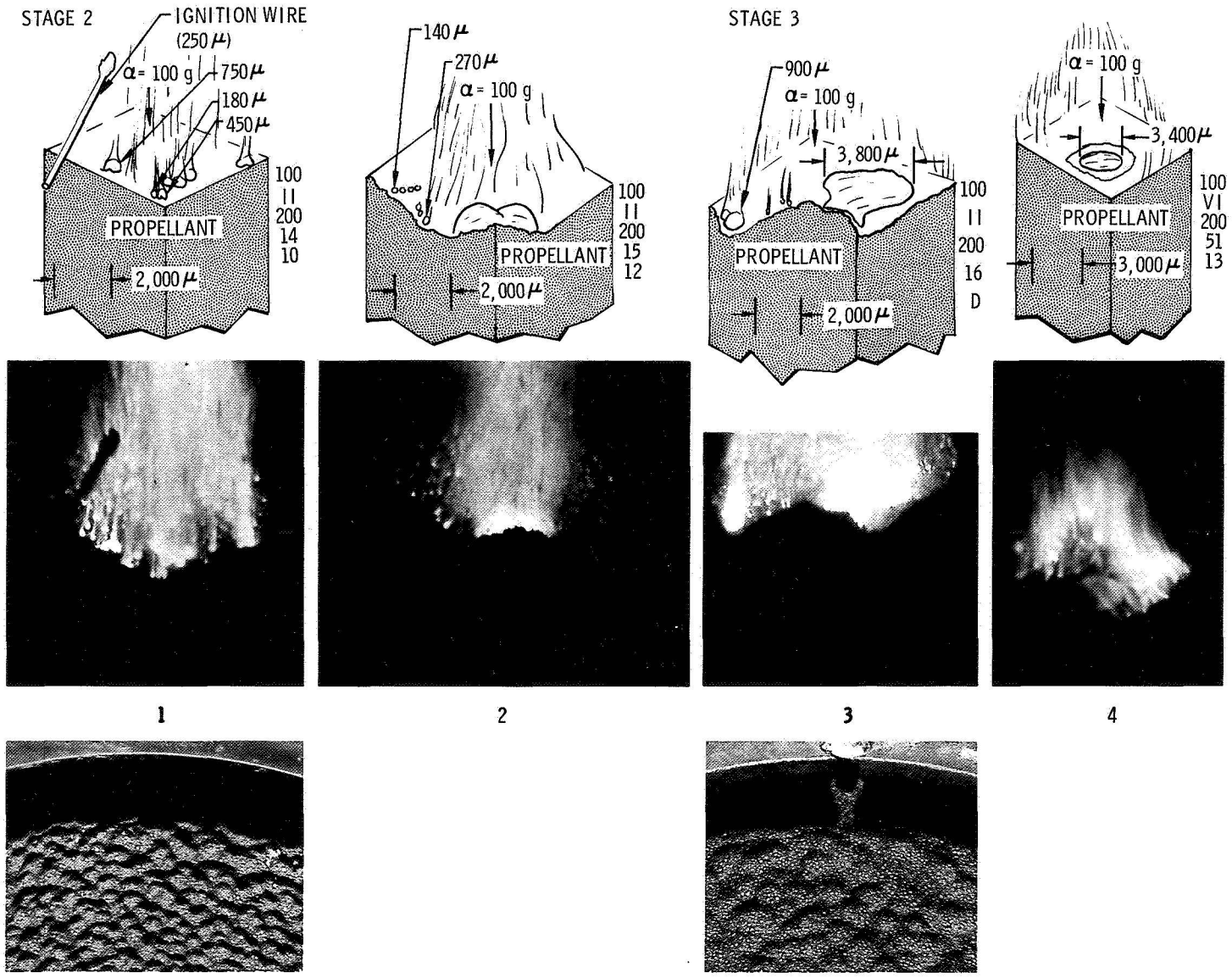

Figure 9. PHOTOGRAPHS AND SCHEMATIC DIAGRAMS OF BURNING PROPELLANTS AND EXTINGUISHED GRAIN SURFACES

91493

burning surface. Selected frames from the films are presented in figure 10. In frame 10-1 a number of small agglomerates can be seen burning on and above the burning surface. The films indicate that combustion under static conditions was not influenced by the 15^{o} angle. At 100 g and 500 psi the agglomerates forming on the propellant surface were almost twice as large as those observed under static conditions (205μ versus 127μ, see table III) and were observed to move down along the 15^{o} incline and fall off the surface of the strand, as shown in frame 10-2. As the agglomerates moved down the surface they appeared to pick up more aluminum and grew to a mass median diameter of 263μ (table III). There was little or no tendency for pits to form in the surface. However, at 100 g and 200 psi, pits formed in the surface and combustion proceeded through stage 1 to stage 2 as described above. A few agglomerates moved off the surface but the majority remained and contributed to the process of pit growth, as seen in frame 10-3. An explanation for the observation that pits formed at 200 psi but not at 500 psi is suggested by the agglomerate size data presented in table III, which shows that agglomerate size increases significantly with decreasing pressure. At 500 psia the agglomerates emerging from the propellant surface were apparently too small to be held on the sloping strand surface by the acceleration forces, while at 200 psi the larger agglomerates were held on the surface and formed pits.

Additional information on the effect of angle was obtained during one test (film No. 5) in which a 1.5-in.-long sample of the control propellant, propellant I, ignited improperly. By chance, this resulted in a burning surface that was inclined at a very steep angle, approximately 30^{o} with respect to the acceleration vector, and a large slag was observed quickly building up on the mounting post. This indicates that grain designs incorporating inclined surfaces, such as star shapes, in spinning propulsion systems may lead to excessive localized slag deposition resulting in case burn-through. The test results obtained with the propellant having small ammonium perchlorate, propellant II, also indicate that pressure is important in determining the influence of the orientation of the acceleration vector on propellant combustion.

4.2 EFFECT OF PROPELLANT FORMULATION, PRESSURE, AND ACCELERATION LEVEL

Even though the phenomena discussed in section 4.1 were common to the majority of the experiments, notable differences were observed between the various propellants and between various pressure and acceleration levels. While the spin sensitivity of aluminized propellants was always controlled by the formation and growth of pits in the propellant surface, the acceleration and pressure levels and the propellant formulation variables determined the size distribution of the aluminum agglomerates. This, in turn, determined the number of pits formed and the rate at which pit growth progressed through the stages described in section 4.1.

Aluminum agglomerate size distributions were measured on films made of propellants I through IV at various pressures. Representative frames were projected on a paper screen, all distinguishable agglomerates were circled, and their size was measured with a Zeiss Particle Size Analyzer, model TGZ-3. A computer program was used to reduce the raw data to number and mass distributions. Between 500 and 1,000 particles were counted in each film, using as many frames as necessary. The selection of agglomerates and

the determination of their diameter required the use of considerable judgment by the investigators;* therefore, the absolute values reported have only limited significance. However, the differences between propellants and the trends with pressure and acceleration level that were observed are believed to be reliable.

The agglomerate size distributions for propellants I through IV burning at 200 psi under static conditions are shown in figure 11. Mass median diameters of the agglomerates observed for propellants I through IV at 200 psi and for propellants I and II at various pressures are presented in table III. The mass median diameter of 438μ for the low burning rate polyurethane propellant IV, compared with 171μ for propellant II with small ammonium perchlorate, shows a marked dependence of agglomerate size distribution upon propellant formulation. The results for the control propellant I and the small ammonium perchlorate propellant also show that agglomerate size decreased with increasing pressure. The single result for propellant II at 100 g indicates an increase in agglomerate size with acceleration.

The fraction of the aluminum content of the propellants as cast, which is represented by these distributions, is not known. The combustion of single or small coalesced aluminum particles was evidenced by many short bright flashes in the high-speed films. Even though it was impossible to quantitatively determine the percentage of aluminum measured in these distributions, a previous study of similar composite propellants at UTC indicated that more than 70% of the initial aluminum was being measured.[12] This estimate was made by comparing the distribution of the initial aluminum cast in the propellant with the agglomerate distribution measured.

In figure 12 the average burning rate augmentation factor is plotted versus acceleration level for propellants I through IV. This factor was determined from subscale motor firing data for internal burners spinning at a constant speed.[2] The magnitude of the augmentation factor and its dependence on acceleration seem to correlate with the agglomerate size distributions: propellants with larger agglomerate size exhibited higher burning rate augmentation factors, that is, increased sensitivity to spin. The data for propellants I, II, and III were obtained in motors with 0.6-in. webs; because the acceleration levels were below 100 g and the pressures below 1,000 psi, pit development never reached stage 5. The motor firing and agglomerate distribution data correlate well, even though the particle size measurements were made on propellants burning under constant pressure and acceleration while the motor data represent averages over the changing pressure and acceleration levels during a firing. A more detailed evaluation of the motor data is not possible because of the dependence of agglomerate size distribution upon both acceleration and pressure level.

The fact that the burning rate augmentation factor changes less with acceleration for the propellants with small ammonium perchlorate and small aluminum, propellants II and III respectively, than for the

* In all cases the particles were easily distinguished while the film projector was in motion; however, when the film was stopped and a single frame projected for analysis it was often difficult to discriminate between the actual particle diameter and the apparent diameter due to the luminosity of the flame. This problem was more severe at higher pressures. An additional problem was the presence of oxide caps on many of the large particles.

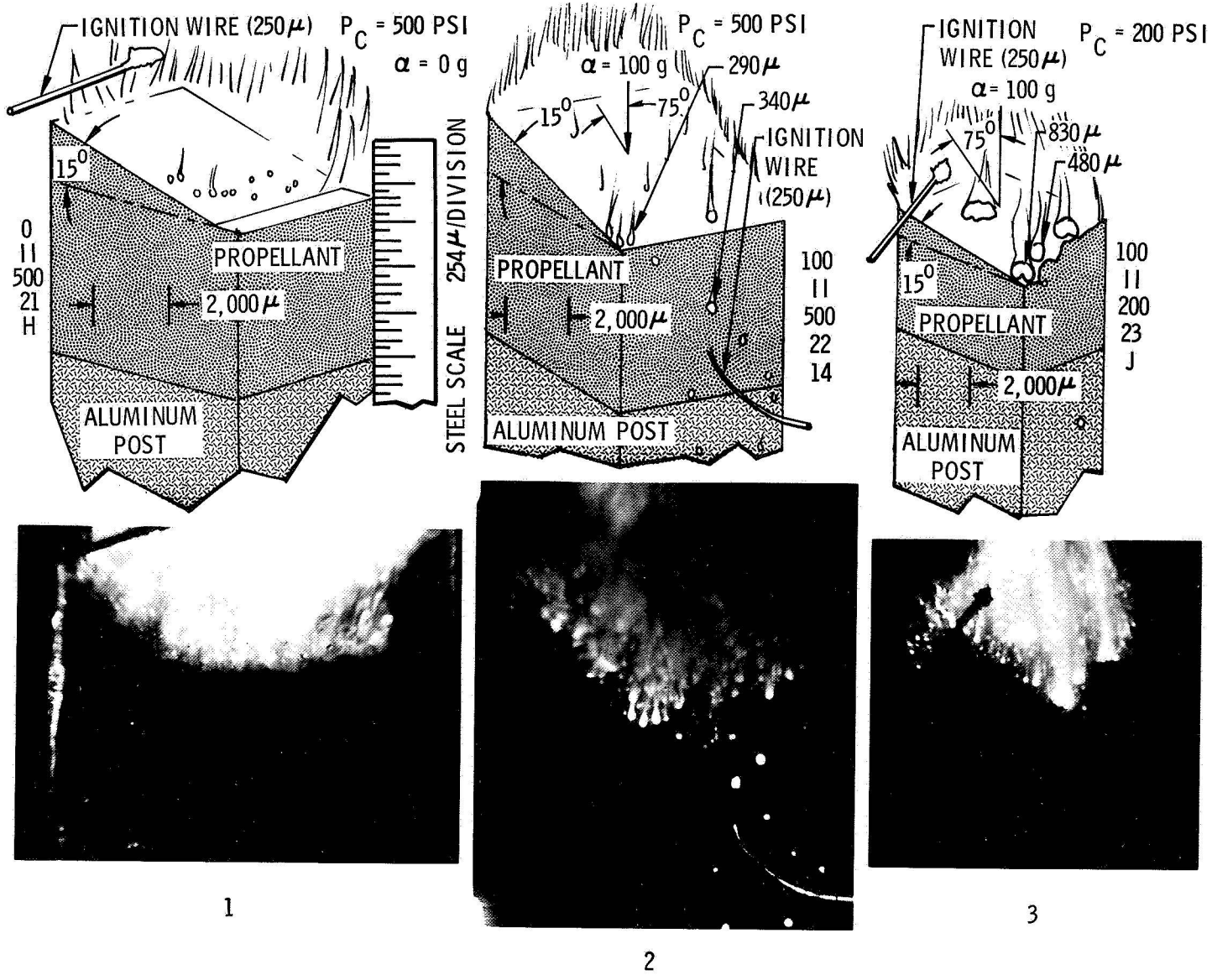

Figure 10. PHOTOGRAPHS AND SCHEMATIC DIAGRAMS OF THE PROPELLANT CONTAINING SMALL AMMONIUM PERCHLORATE (PROPELLANT II) BURNING UNDER STATIC AND ACCELERATION CONDITIONS WITH THE ACCELERATION VECTOR ORIENTED AT 75° TO THE BURNING SURFACE

91494

TABLE III

MASS AND NUMBER MEDIAN DIAMETERS OF AGGLOMERATES
ON OR IMMEDIATELY ABOVE THE PROPELLANT SURFACE

Propellant	Diameter, μ					
	Pressure, psi					
	200		500		1,000	
	D_m	D_n	D_m	D_n	D_m	D_n
I (Control)	327	184	306	182	150	103
II (Small Ammonium Perchlorate)	171	116	127 205* 263†	93 140 176	–	–
III (Small Aluminum)	225	126	–	–	–	–
IV (Polyurethane)	438	181		–	–	–

* α = 100 g

† α = 100 g at 75° with respect to surface, agglomerates rolling off edge of strand

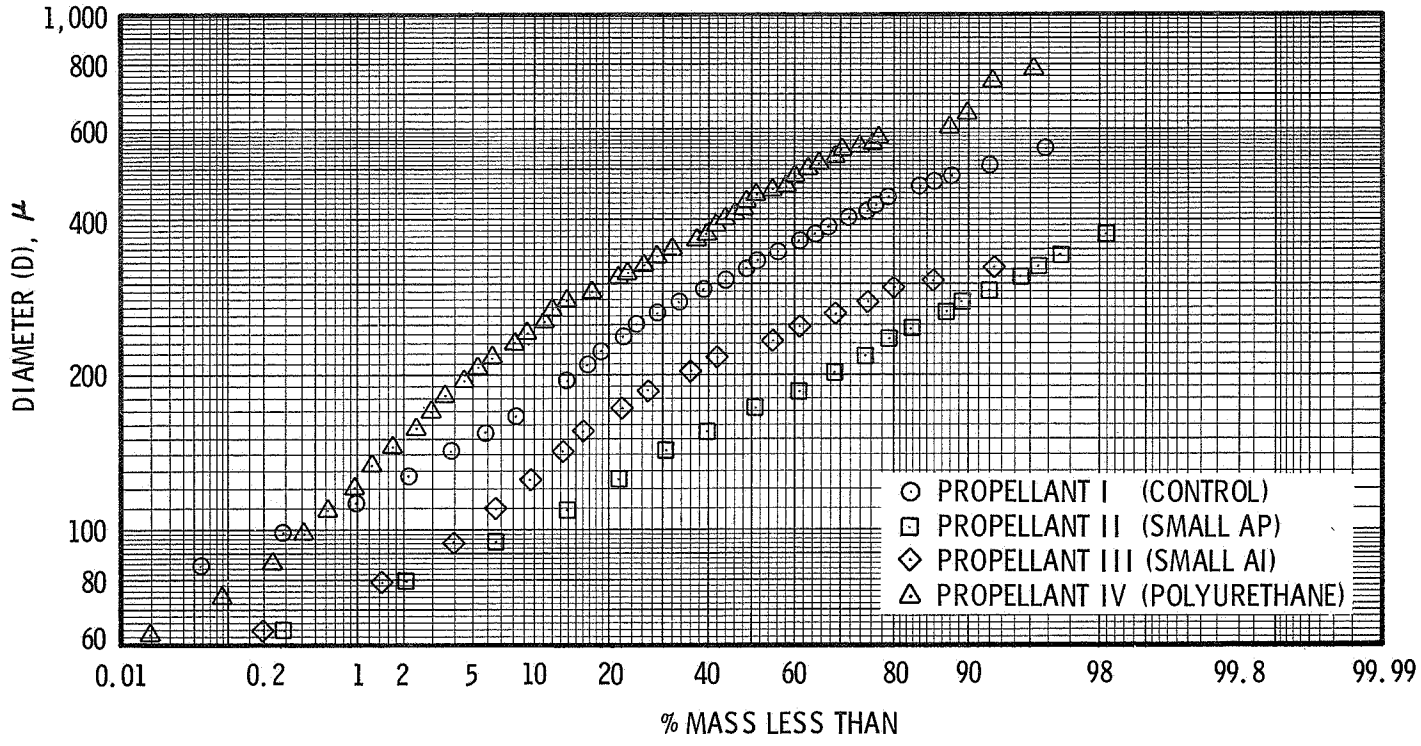

Figure 11. Agglomerate Size Distribution for Propellants I Through IV Burning at 200 psi

91495

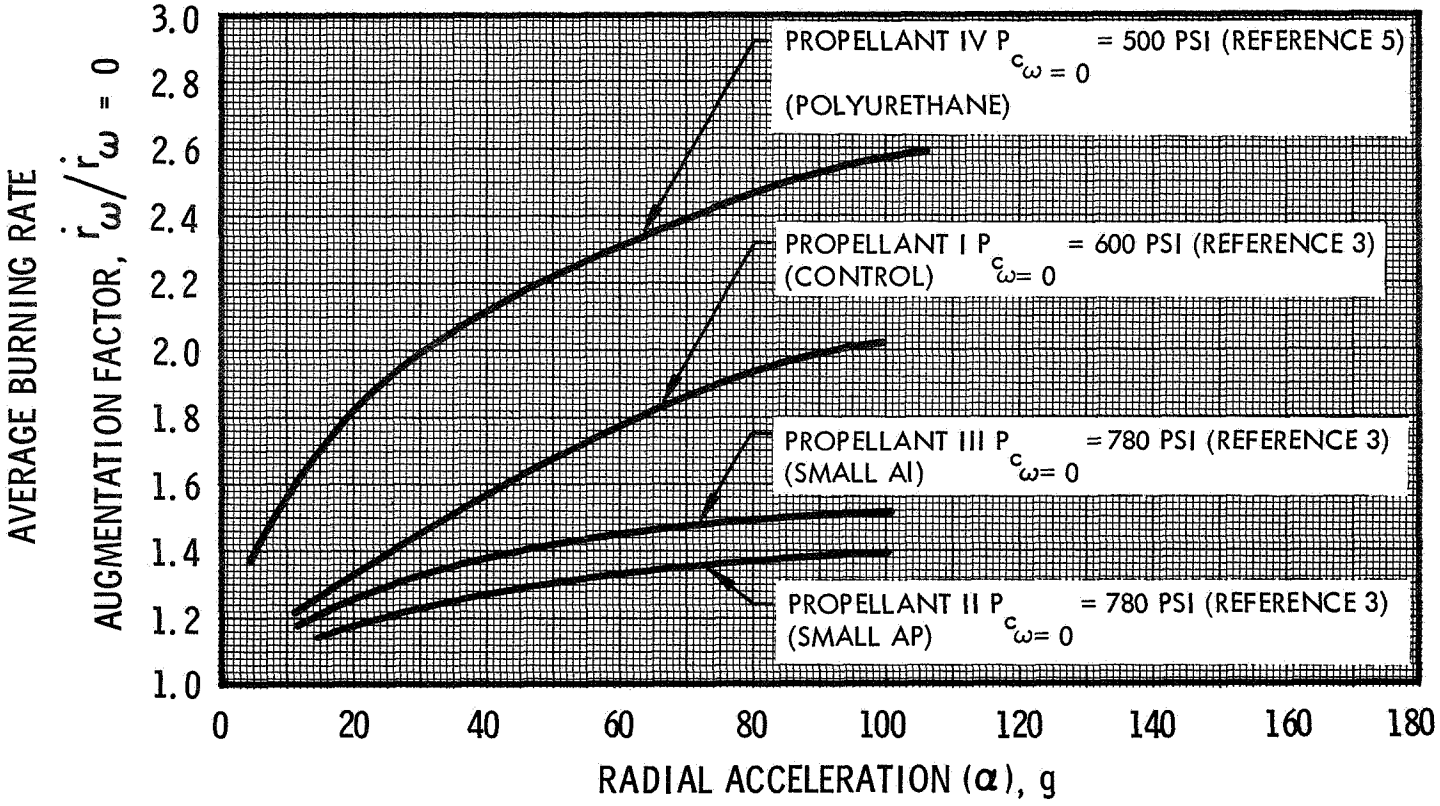

Figure 12. Motor Data for Average Burning Rate Augmentation Factor vs Radial Acceleration for Propellants I Through IV

91496

control propellant, indicates a significant difference in the processes occurring at the burning surface. It was noted in the films that propellants II and III progressed to stage 3 combustion much more quickly than propellant I. Figures 13 and 14 illustrate, respectively, the control propellant and propellant III with small aluminum. Frame 1 in each figure shows the propellant burning under static conditions with 200μ- to 400μ-diameter aluminum agglomerates burning on or near the surface. The larger size of the agglomerates from propellant I is apparent. Frame 2 in each figure shows the propellant burning at 100 g, after about 1/8 in. of the strand had burned away. At this time, propellant I had formed a large number of pits containing 200μ- to 800μ-diameter spherical globules characteristic of stage 2 combustion. Propellant III, in frame 14-2, exhibits the larger button-shaped globules of 800μ- to 1,000μ-diameter characteristic of stage 3 combustion. Propellant II showed a similar behavior. The films indicate that this difference in transient behavior was due to a higher density of pits resulting from the larger number of small agglomerates in the case of propellants II and III. This seemed to facilitate the transition to stage 3 combustion, whereas propellant I, with larger agglomerates and a smaller number of large pits, required additional time to form the long shallow pits characteristic of stage 3.

An agglomerate size distribution is not presented for propellant V containing the magnesium/aluminum alloy because the agglomerates were too small to be measured. Propellant V did not exhibit any sensitivity to acceleration at pressures up to 1,000 psi and acceleration levels of 100 g. Agglomerates never appeared on the surface, and in one test at 100 g and 200 psi (film No. 44), even pieces of the igniter wire that were retained on the surface did not form pits.

Figure 15 shows a comparison between propellant V and the low burning rate polyurethane propellant IV under static and acceleration conditions. Large agglomerates (200μ- to 500μ-diameter) may be seen on and above the surface of propellant IV in frame 15-1, while no agglomerates may be seen on the surface of propellant V, frame 15-3. When the propellants were burning under acceleration, large globules between 800μ and 1,500μ in diameter were seen on the surface of propellant IV (frame 14-2), while the burning surface of propellant V does not exhibit any change with acceleration (frame 14-4). Further evidence of the absence of agglomerate formation during the combustion of propellant V is provided by the fact that no particles are falling off the burning surface on the side of the strand, as was observed when strands of any of the other propellants ignited on the side.

In addition to the effect of pressure on agglomerate size, the Al/Al_2O_3 agglomerates on the surface of the propellants burning under acceleration appeared to be more fluid at 1,000 psi than at the lower pressures and in some instances bored small deep holes in the surface. Apparently they had a higher temperature, which is also borne out by a large increase in the luminosity of the individual agglomerates as the pressure increased, making necessary a decrease in film exposure. At high pressure the total radiation was also increased by the increased density of Al_2O_3 in the combustion gases immediately above the burning surface. The increased brightness and total radiation reduced the overall quality of the films and limited the area of the strand surface which could be seen.

While it was not possible to quantitatively measure the increase in temperature, the film records of all tests made at high pressure confirm its presence. Because the propellant equilibrium flame temperature is almost constant above 200 psi, the increase in brightness cannot be attributed to variations in the final combustion temperature; however, equilibrium vaporization calculations for Al_2O_3 suggest that the

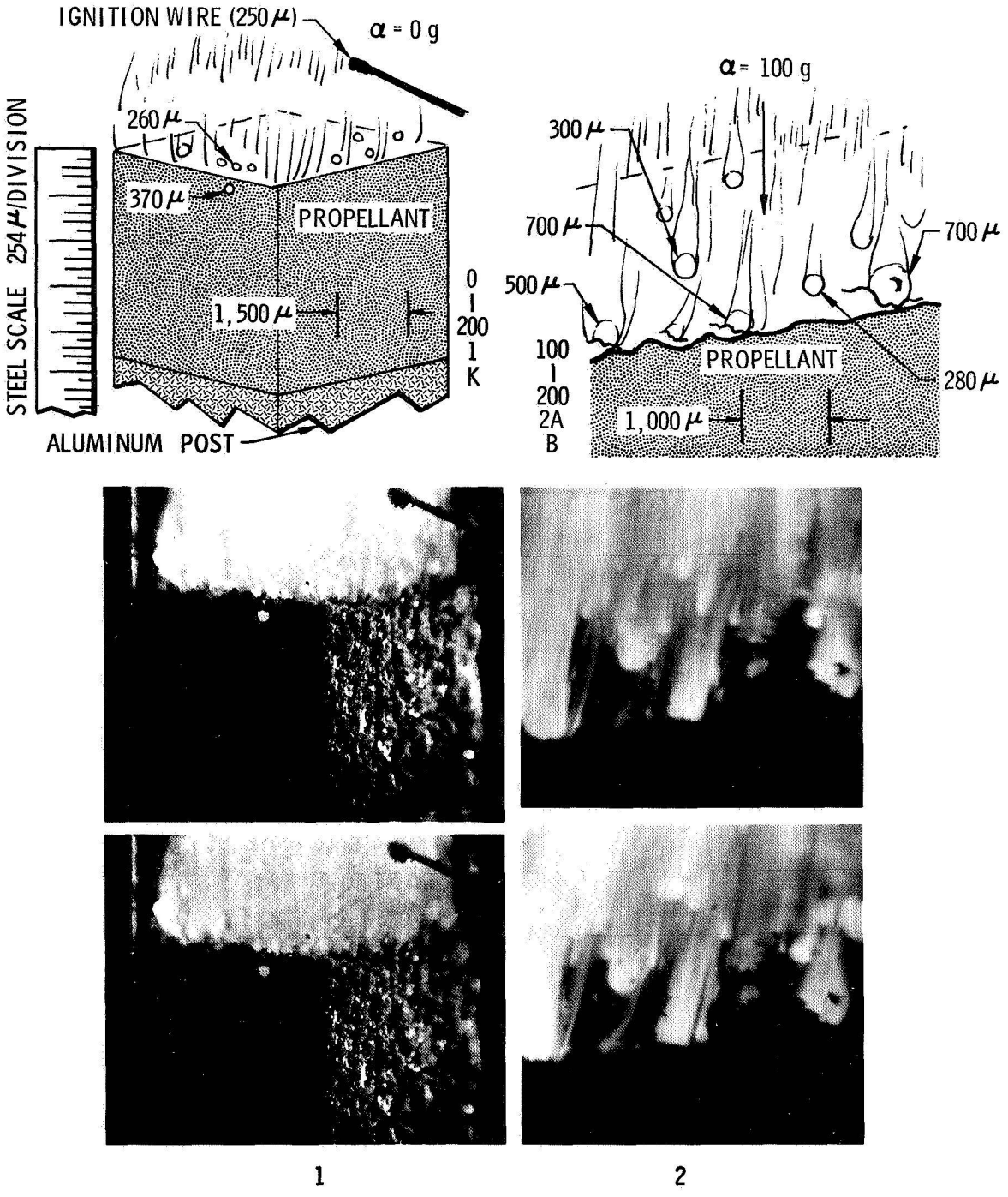

Figure 13. PHOTOGRAPHS AND SCHEMATIC DIAGRAMS OF CONTROL PROPELLANT (PROPELLANT I) BURNING AT 200 PSI UNDER STATIC AND ACCELERATION CONDITIONS

91497

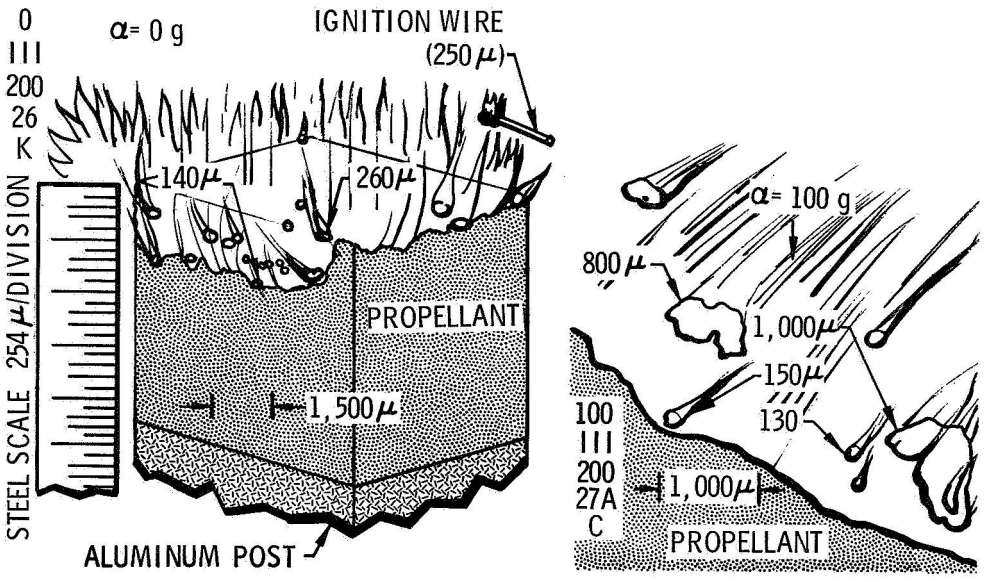

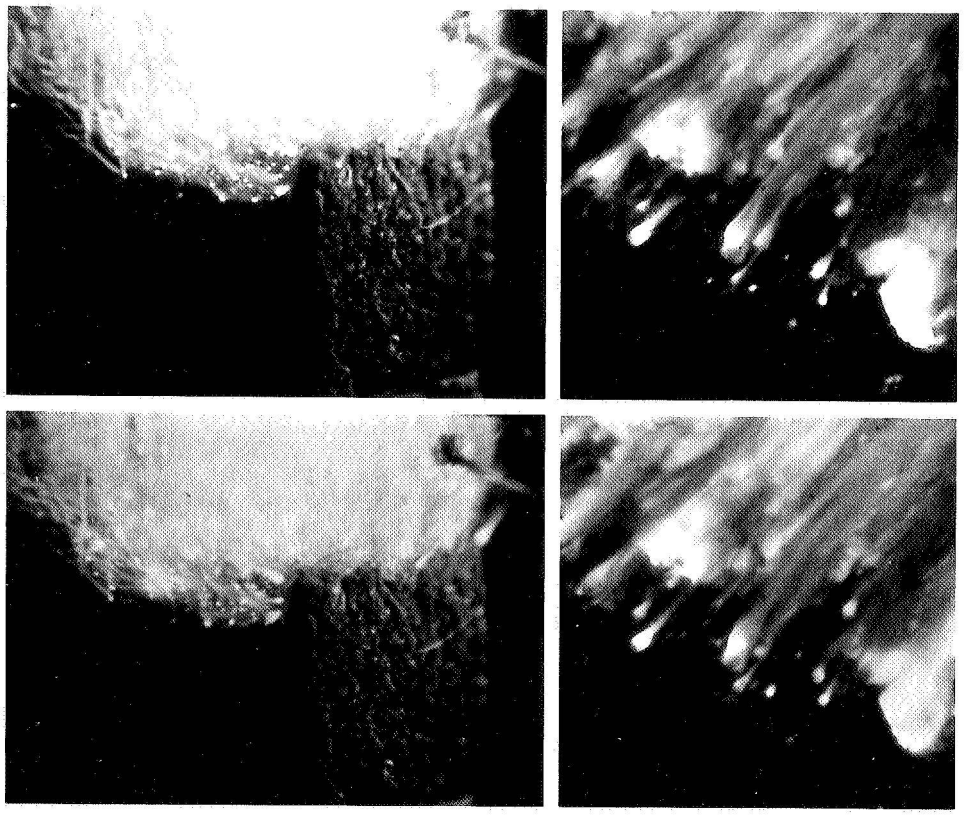

1 2

Figure 14. PHOTOGRAPHS AND SCHEMATIC DIAGRAMS OF PROPELLANT CONTAINING SMALL ALUMINUM (PROPELLANT III) BURNING UNDER STATIC AND ACCELERATION CONDITIONS

91498

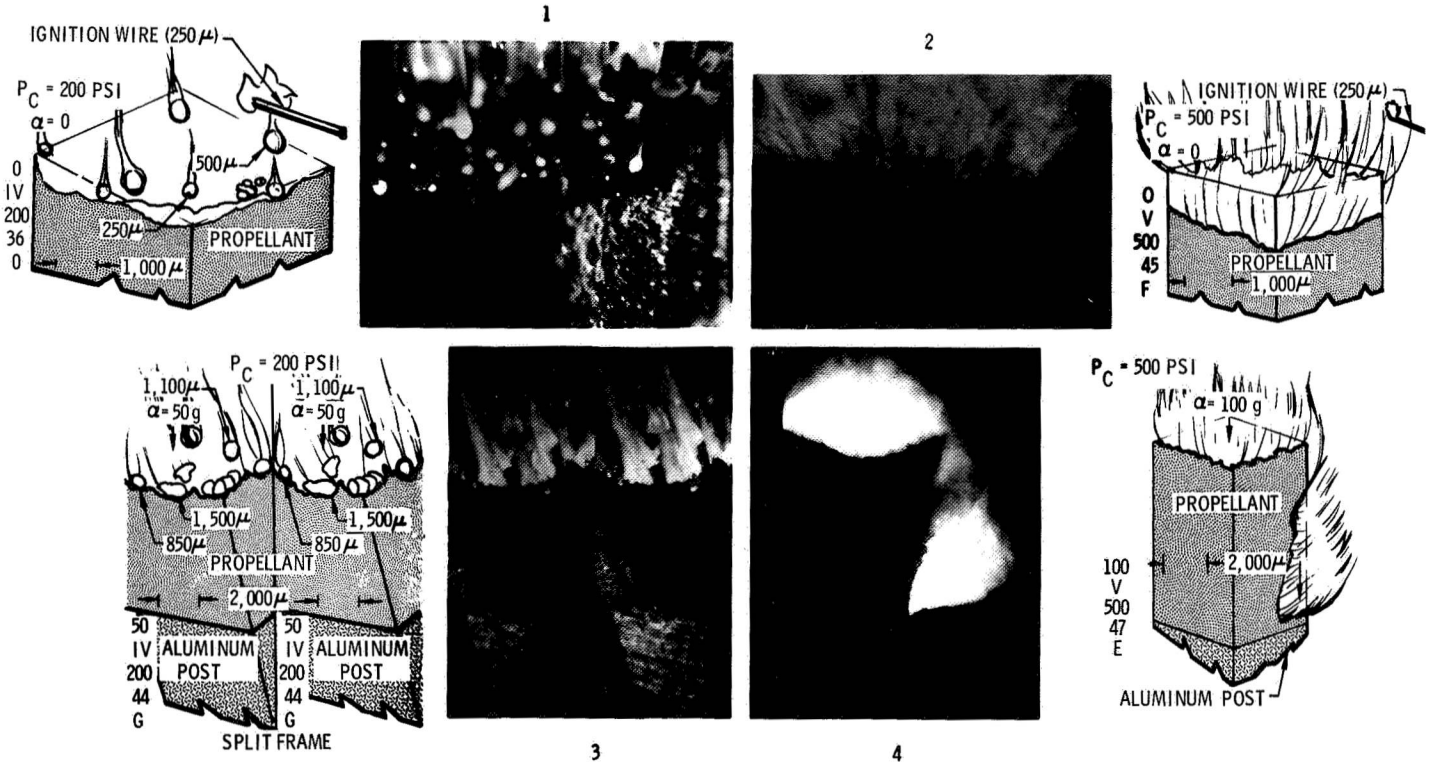

Figure 15. PHOTOGRAPHS AND SCHEMATIC DIAGRAMS OF POLYURETHANE PROPELLANT (PROPELLANT IV) AND PROPELLANT WITH THE MAGNESIUM/ALUMINUM FUEL (PROPELLANT V)

91499

agglomerate temperature may increase as much as 500°K from 200 to 1,000 psi. One other notable effect of high pressure was that the burning surface became very rough; the ammonium perchlorate appeared to regress faster than the binder, leaving small fingers of binder projecting from the surface.

These studies indicate that the strength of the acceleration field determines the number and total mass of aluminum agglomerates retained on the burning surface. The number of these agglomerates determines the initial pit density, and the total mass retained controls the magnitude of the spin-augmented burning rate. The films show that the initial pit density appeared to determine the time required to progress from stage 1 to stage 3 of the combustion process. Once stage 3 combustion had been reached, almost all of the aluminum evolving from the propellant was captured by the large Al/Al_2O_3 globules on the surface and further transient behavior was influenced less by pressure, acceleration level, and propellant formulation. The films indicate that propellant II with small ammonium perchlorate and propellant III with small aluminum very quickly proceeded to stage 3 combustion. They were both characterized by a considerable amount of single-particle aluminum combustion above the surface and by the early development of numerous small pits. The control propellant I and the low burning rate polyurethane propellant IV, on the other hand, required considerably more time to proceed to stage 3; the aluminum appeared to be retained on the surface in a smaller number of relatively large pits. The motor firing data shown in figure 14 reflect these observations: propellants I and IV exhibit large spin-augmented burning rates which vary appreciably with acceleration level, while propellants II and III show lower augmented burning rates and less change with acceleration level.

All the above results confirm that combustion under acceleration proceeds through stages 1 through 5, as described in section 4.1 and that the time required to reach a given stage is dependent upon propellant formulation, operating pressure, and acceleration level.

4.3 EXTINGUISHED PROPELLANTS AND ALUMINUM AGGLOMERATES

The character of the Al/Al_2O_3 slag retained on the sample mounting post at burnout was similar to that found in previous postfire observations of spin motor propellant cases.[3] In some of the films a large globule could be observed cooling to its final shape on the mounting post (see figure 9-4), which provided a positive correlation between the stage of combustion and the shape and size of the residual slag particle. The films also showed that the particle cooled very quickly as it came to rest upon the aluminum mounting post.

Quenched residues obtained from each propellant under a variety of operating pressures and acceleration levels were studied and photographed with a scanning electron microscope after they had been coated with a thin layer of vapor-deposited gold.* The residue from all samples was similar to that shown in figure 16. A typical sample contained a large globule 500μ to 5,000μ in diameter (micrographs 16-1 and 16-2) surrounded by residue similar to that shown in micrograph 16-4. Because the large globule was burning in a pit, it reached the post and cooled before the surrounding propellant was consumed, as shown in figure 9-4. The continuing combustion is believed to be the reason for the small particles found on the

* All scanning electron photomicrographs were taken by Applied Space Products, Inc., Palo Alto, California.

surface of the large globule, as shown in figure 16-3. A number of small holes, which were probably formed by gases escaping as the globule cooled, are visible on the surfaces of the large globules.

Photomicrographs of a 3,000μ-diameter particle which resulted from the combustion of a 1-in.-long sample of propellant II with the small ammonium perchlorate, burning at 200 psi and 100 g, are shown in figure 17. This particle was selected from film No. 15, which illustrates combustion in stage 3 with exceptional clarity. The surface of the particle is shown in micrographs 17-1 and 17-3; and micrographs 17-2 and 17-4 show details of holes found in the surface of the particle. Tubular voids were found in the interior of the globule, as shown in micrograph 17-6, and additional details of the interiors of the voids are shown in micrographs 17-7 and 17-8. The walls of the voids are smooth with attached particles which appear to have condensed or to have been extruded as the globule cooled. The bright appearance of these particles may be due to the sample preparation procedure used and does not necessarily signify a difference in composition. The top edge of the particle was examined to find an exposed hole similar to those found in the surface; micrograph 17-5 shows a representative vent hole.

The tubular voids and vent holes in the residual slag globule indicate the presence of aluminum vapor or other gaseous species inside the globule prior to quench. After the scanning electron photomicrographs were obtained, a review of film No. 15 revealed that jets of gas or vapor seemed to issue from the globule periodically during combustion.

Scanning electron photomicrographs were also taken of extinguished propellant surfaces, agglomerates which had fallen from the propellant surface during combustion, and samples of the aluminum particles cast in the propellant. The circular areas shown in the photomicrographs of the extinguished grain surfaces (micrographs 18-1 and 18-2) are believed to be the surfaces of partially decomposed ammonium perchlorate particles. The appearance of these particles suggests the subsurface evolution of gas and the existence of a liquid surface layer during combustion. The agglomerates shown in micrograph 18-5 fell from a strand burning under acceleration and were collected from the base of the combustion bomb after the experiment. Those in the foreground of the photo appear to have a sintered structure and were probably quenched during their formation. The particle in the center rear has coalesced and is similar in appearance to particles of the original aluminum cast in the propellant (see micrograph 18-6) except that its diameter is larger by a factor 7. The diameter of the larger particles, approximately 150μ, agrees well with that of the burning particles leaving the propellant surface.

The original aluminum particles cast in propellants I, II, and III were spherical; attached to all the larger particles were a number of smaller particles, as shown in micrograph 18-6. These smaller particles may play an important role in the sintering process in which the agglomerates first form, since they would tend to melt and ignite much faster than their parent particles.

The high-magnification photos with the remarkable depth of field provided by the scanning electron microscope provide valuable information. Unfortunately, this technique provides no means to distinguish between various materials in the sample, such as aluminum and Al_2O_3.

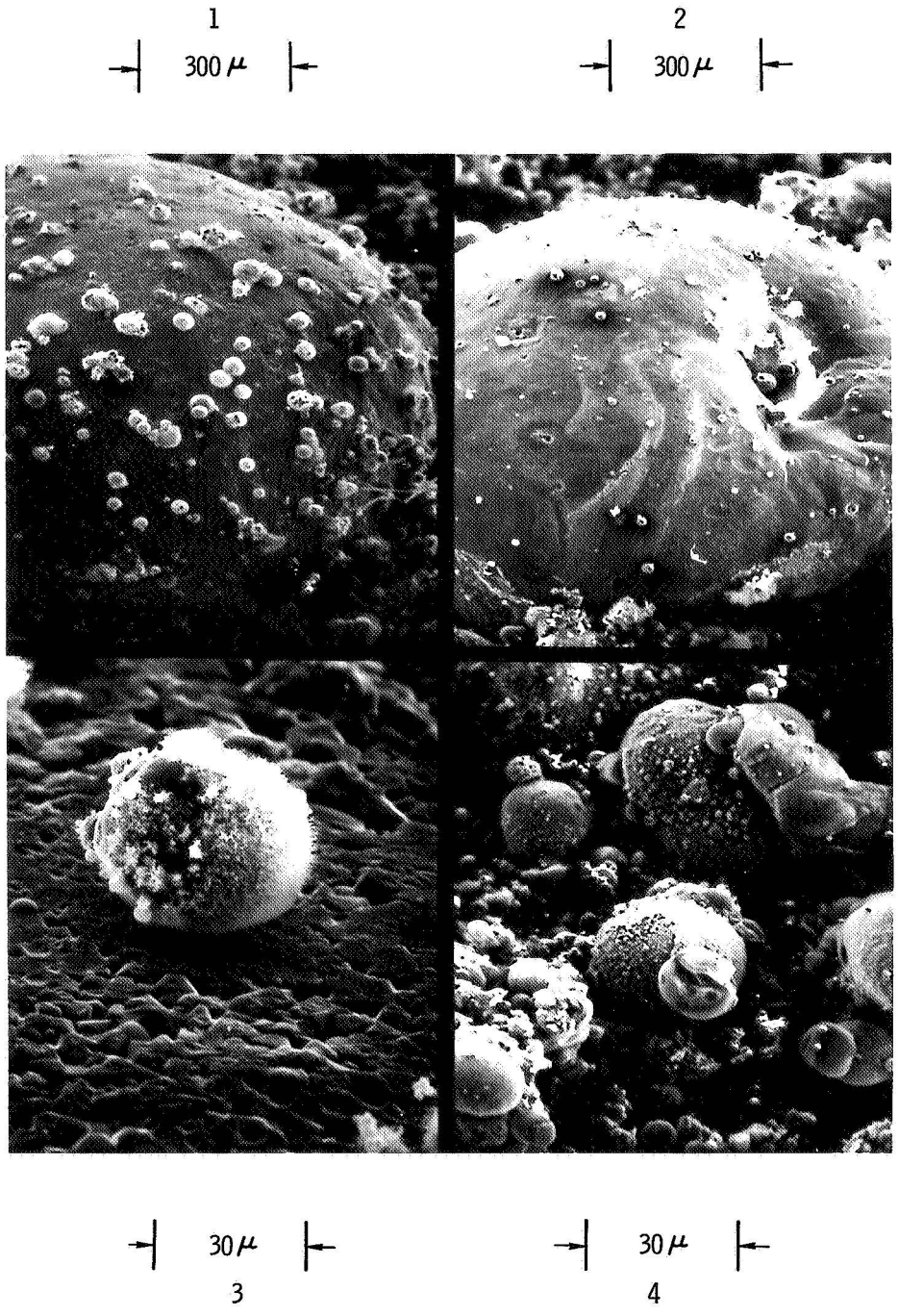

Figure 16. SCANNING ELECTRON MICROGRAPHS OF RESIDUAL SLAG

91500

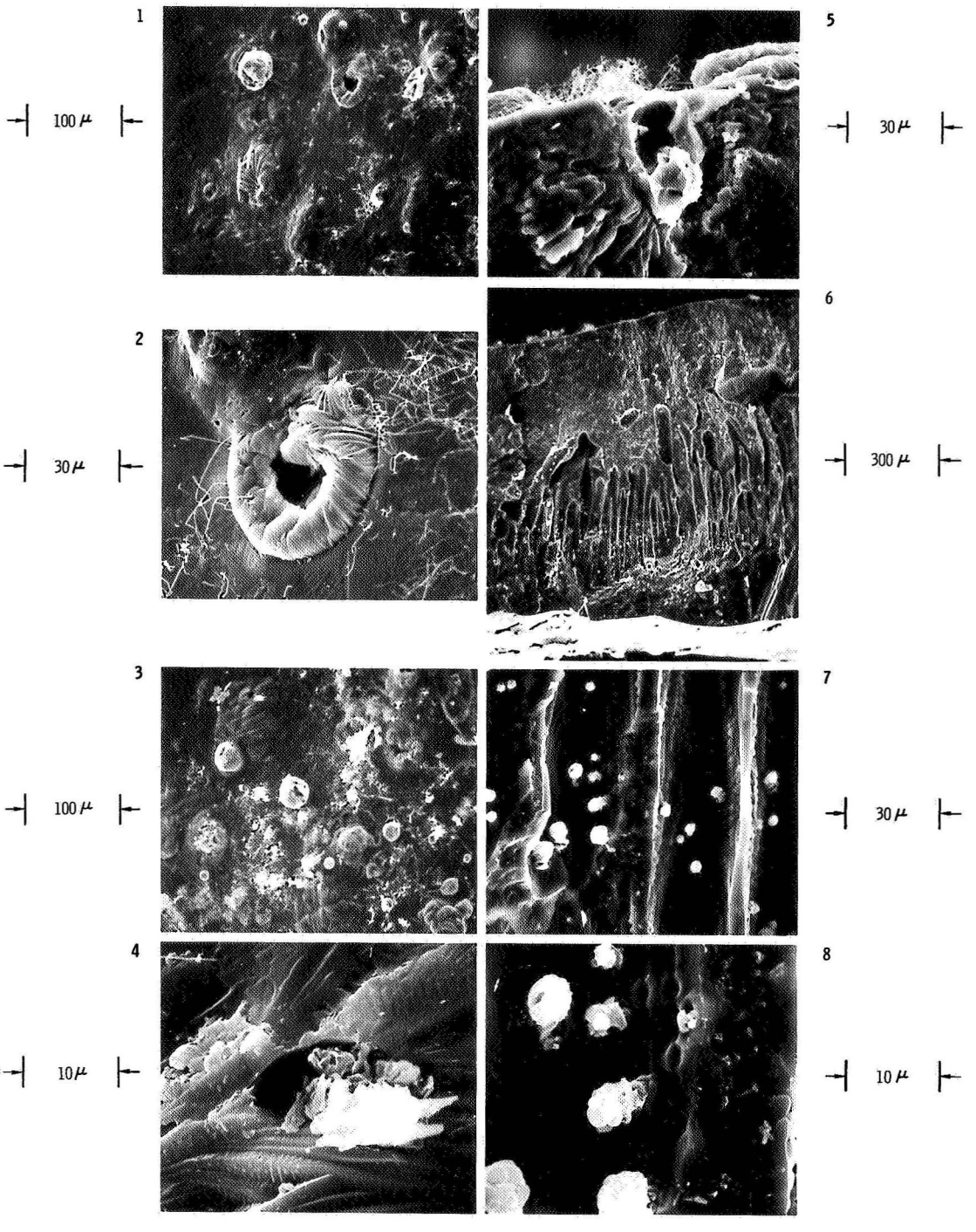

Figure 17. SCANNING ELECTRON MICROGRAPHS OF A SINGLE SLAG PARTICLE RESULTING FROM STAGE 3 COMBUSTION

91501

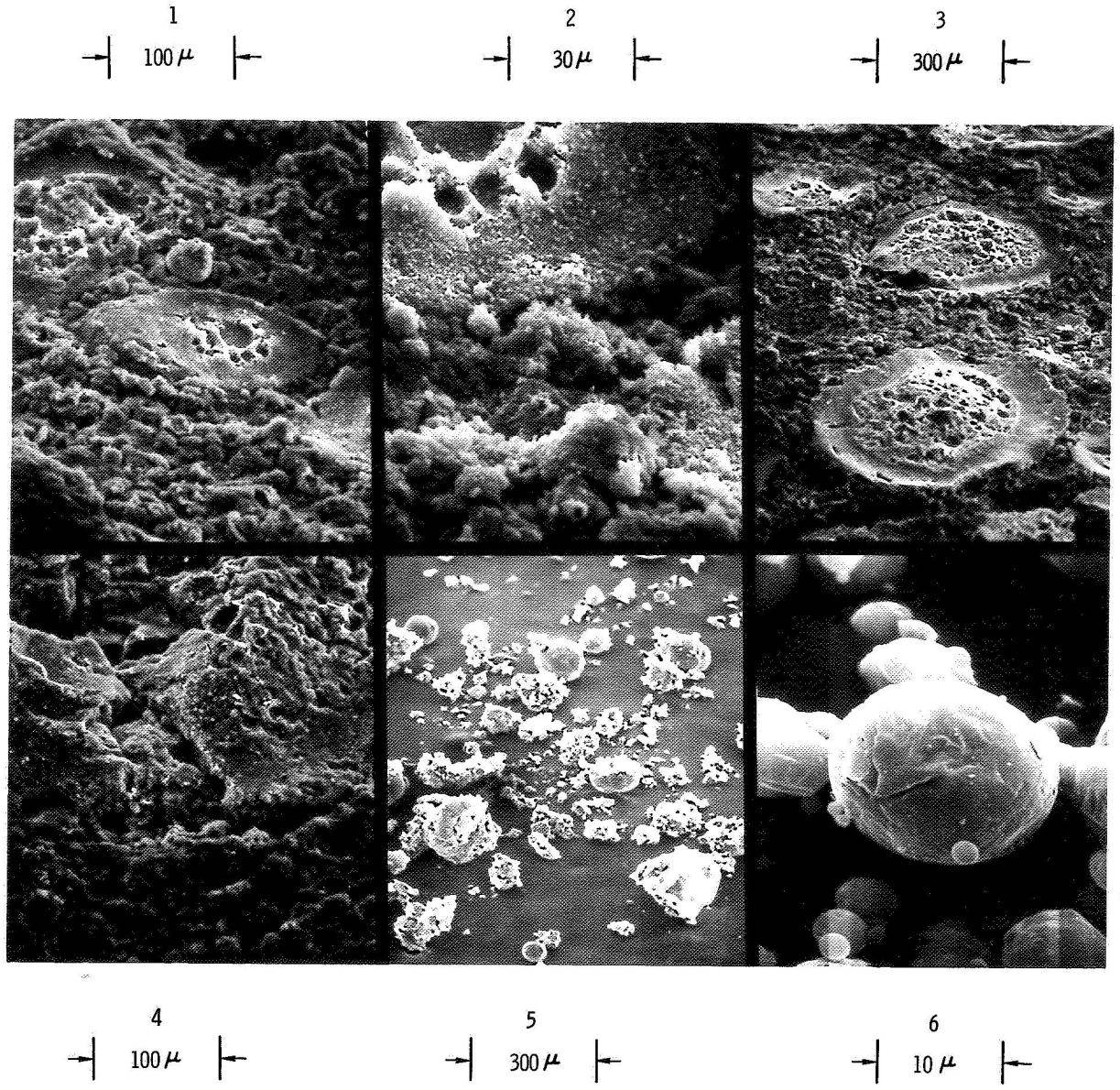

Figure 18. SCANNING ELECTRON MICROGRAPHS OF EXTINGUISHED GRAIN SURFACES AND ALUMINUM PARTICLES

91502

5.0 DESCRIPTION OF EDITED FILM

The experimental program included high-speed color photography of six propellants burning under the various conditions of pressure and acceleration listed in table II. The film from each experiment was critically reviewed, and an 18-ft clip (720 frames) representative of the entire film was selected for inclusion in a composite film; the composite is approximately 1,200 ft long. It begins with a short documentary on the experimental apparatus* followed by the edited film clips of each experiment including test and propellant information. The order of the film clips in the final film is shown in table IV together with the corresponding experimental conditions.

Each film clip provides 30 sec of viewing time at the standard projection speed of 24 frames/sec, or 45 sec of viewing time at 16 frames/sec. These viewing times are adequate for a qualitative comparison of adjacent film clips; detailed analyses of the films may be carried out using a projector with a single frame and very slow framing rate features.† While the film clips were selected as representative, the complete film of a particular experiment may be required to observe the complete history of pit formation. Copies of the edited film are available on loan from Langley Research Center and may be obtained by submitting the request form shown at the end of this report. The complete set of original films is on permanent file at UTC.

To fully appreciate the edited film, the observer should remember the following items:

A. Because the camera was stationary and the centrifuge table rotated during the test, the image of the burning propellant sample will slowly rotate as the film is projected.

B. The acceleration vector is always directed at 90° to and into the burning propellant surface regardless of the apparent orientation of the surface, except in films No. 22 and 23 where the acceleration vector is at 75°.

C. The N_2 purge gas used to keep the observation window free from smoke is directed away from the propellant surface, that is, opposite the acceleration vector.

D. In all cases the sample is viewed at 13° to the burning surface, with the camera focused approximately 0.15 in. above the mounting post and 0.12 in. in from the front corner, as shown in figure 6.

E. Films clips of tests made at 500 and 1,000 psi do not, in general, provide as much information as those made at 200 psi because the increased pressure resulted in greater particle density and some overexposure.

F. For the long strands used in films No. 3, 4, 5, 15, 16, 28, 29, and 52, only the last one-quarter of the burning strand was photographed.

---

* In the film the camera is shown mounted horizontally; however, for the work reported here, it was mounted directly above the spin table as shown in figure 3.

† The analyses in this report were carried out using a L & W Photo, Inc., model 224A Photo-Optical Data Analyzer.

TABLE IV

TABULATION OF HIGH-SPEED FILMS, TEST AND PROPELLANT INFORMATION

Film Number	Propellant	Test No.	Combustion Pressure psia	Acceleration g	Pictures per second	Magnification	Strand Length in.
1	I	3/4-1	200	0	3.10 K	0.77	0.25
2	I	3/20-1	200	100	2.20 K	0.80	0.25
2A	I	6/6-3	200	100	5.50 K	1.75	0.22
3	I	3/24-1	200	100	1.15 K	0.80	1.00
4	I	4/18-5	200	100	10.00 K	0.55	1.00
5	I	3/21-3	200	100	1.10 K	0.80	1.50
6	I	2/27-2	500	0	3.00 K	0.47	0.25
7	I	12/30-2	500	25	2.70 K	0.80	0.25
8	I	12/18-2	500	50	2.70 K	0.80	0.25
9	I	12/18-1	500	75	2.70 K	0.80	0.25
10	I	12/30-3	500	100	2.61 K	0.80	0.25
11	I	3/12-1	1,000	0	3.30 K	0.84	0.25
12	I	4/17-4	1,000	100	5.00 K	0.55	0.40
13	II	3/4-2	200	0	3.50 K	0.77	0.25
14	II	3/21-2	200	100	2.70 K	0.80	0.28
14A	II	6/6-1	200	100	6.10 K	1.75	0.22
15	II	3/24-2	200	100	1.10 K	0.80	1.00
16	II	4/18-4	200	100	10.00 K	0.55	1.00
17	II	2/27-3	500	0	3.20 K	0.47	0.25
18	II	12/30-5	500	25	2.60 K	0.80	0.25
19	II	12/24-1	500	50	2.80 K	0.80	0.25
20	II	12/24-2	500	100	2.90 K	0.80	0.25
21	II	3/12-4	500	0*	3.70 K	0.84	0.25
22	II	1/2-2	500	100*	2.70 K	0.84	0.25
23	II	3/20-2	200	100*	2.90 K	0.80	0.25
24	II	3/4-5	1,000	0	3.60 K	0.77	0.25
25	II	4/17-2	1,000	100	5.00 K	0.55	0.50
26	III	3/4-3	200	0	3.00 K	0.77	0.25
27	III	3/21-1	200	100	2.80 K	0.80	0.30
27A	III	6/6-2	200	100	6.20 K	1.75	0.22
28	III	3/24-3	200	100	1.20 K	0.80	1.00
29	III	4/18-3	200	100	10.00 K	0.55	1.00
30	III	3/12-2	500	0	3.00 K	0.84	0.25
31	III	1/2-4	500	25	2.70 K	0.80	0.25
32	III	12/20-1	500	100	2.70 K	0.80	0.25
33	III	1/2-5	500	100	2.70 K	0.80	0.25

TABLE IV

TABULATION OF HIGH-SPEED FILMS, TEST AND PROPELLANT INFORMATION (Continued)

Film Number	Propellant	Test No.	Combustion Pressure psia	Acceleration g	Pictures per second	Magnification	Strand Length in.
34	III	3/12-3	1,000	0	3.00 K	0.84	0.25
35	III	4/18-1	1,000	100	5.50 K	0.55	0.40
36	IV	4/2-4	200	0	4.10 K	1.00	0.20
37	IV	4/15-2	200	50	10.20 K †	0.55	0.30
38	IV	4/2-5	500	0	3.00 K	1.00	0.20
39	IV	4/15-3	500	50	10.00 K †	0.55	0.30
40	IV	5/6-2	500	100	3.10 K	0.51	0.45
41	IV	4/2-6	1,000	0	3.80 K	1.00	0.20
42	IV	5/16-1	1,000	50	4.80 K	0.51	0.40
43	V	4/2-1	200	0	3.00 K	1.00	0.25
44	V	4/15-1	200	100	6.00 K †	0.55	0.30
45	V	4/2-2	500	0	3.00 K	1.00	0.25
46	V	5/6-3	500	50	3.00 K	0.51	0.45
47	V	5/7-1	500	100	3.10 K	0.51	0.45
48	V	4/2-3	1,000	0	4.70 K	1.00	0.25
49	V	4/17-6	1,000	100	5.00 K	0.55	0.40
50	VI	4/2-7	200	0	3.90 K	0.51	0.45
51	VI	5/6-1	200	100	3.00 K	0.51	0.45
52	VI	5/9-2	200	100	1.60 K	0.51	1.00

* Acceleration vector oriented 75° with respect to the burning surface

† Pictures taken in split-frame mode

PROPELLANT I

16% PBAN Binder

68% AP 65% 400μ
35% 8μ

16% Al 46μ

PROPELLANT II

16% PBAN Binder

68% AP 40% 190μ
60% 8μ

16% Al 46μ

PROPELLANT III

16% PBAN Binder

68% AP 65% 400μ
35% 8μ

16% Al 8μ

PROPELLANT IV

25% Polyurethane

57% AP 200μ

18% Al 26μ

PROPELLANT V

16% CTPB Binder

68% AP 70% 200μ
30% 20μ

16% Mg/Al Alloy

PROPELLANT VI

14% PBAA Binder

70% AP 70% 190μ
30% 20μ

16% Al

6.0 CONCLUSIONS

High-speed color cinematography of aluminized composite solid propellants burning under acceleration and examination of residual slag resulted in the following conclusions:

A. Aluminum agglomerates formed on the burning propellant surface with and without acceleration forces present. When acceleration forces were present, the agglomerates were held on the surface and coalesced into burning globules which formed pits in the propellant surface. As burning proceeded, these pits merged, becoming broader and shallower, and the globules flattened out.

B. The formation and growth of the pits may be described in terms of five stages as follows:

Stage 1	Sites are established on the surface by agglomerates formed shortly after ignition.
Stage 2	The agglomerates coalesce to form large spherical globules under which pits develop.
Stage 3	The pits merge to form broader and shallower pits containing button-shaped Al/Al_2O_3 globules. The globules also grow by the influx of aluminum from the pit walls.
Stage 4 to 5	The pits continue to grow and to become broader and shallower. The button-shaped globules become puddles and finally form a sheet.

C. Combustion of all the aluminized propellants studied proceeded through the five-stage process under acceleration; however, the time required to reach a given stage was dependent upon propellant formulation and on the pressure and acceleration level. The propellant containing a magnesium/aluminum alloy did not exhibit any changes in combustion due to acceleration under the conditions tested.

D. The aluminum agglomerates on the surface had mass median diameters ranging from 130μ to 440μ. Agglomerate size was mainly dependent upon propellant formulation, decreasing with reduced ammonium perchlorate and aluminum size, but also decreasing with pressure and increasing with acceleration level.

E. Spin-augmented burning rates, as determined from spinning solid rocket motor tests, were correlated with agglomerate size data obtained in this study. The results show that increasing agglomerate size corresponds to increasing spin sensitivity.

F. The globules in the form of residual slag were examined with a scanning electron microscope and found to have vent holes in their surface and internal tubular voids indicating the presence of aluminum vapor or other gaseous species prior to quench.

7.0 SUGGESTIONS FOR FURTHER STUDY

The photographic studies conducted under this contract, together with studies recently made at NASA Langley Research Center, provide a reasonably complete qualitative understanding of the transient processes occurring at the burning surface of conventional aluminized solid propellants under acceleration. Analytical studies of aluminum agglomeration, slag buildup, and the formation and growth of pits can now be undertaken to provide a quantitative framework for ballistic design and for the correlation of experimental motor data.

Further experimental data, of the type obtained in this study, should also be obtained for propellants with high static burning rates. Generally, such propellants have been less sensitive to acceleration; however, no studies have been made of the effect of acceleration on very high burning rate propellants which contain special ingredients and probably burn by a mechanism substantially different from that of conventional propellants.

The success of the photographic technique used in this study indicates that it would be useful also for studying the combustion mechanism of solid propellants under static conditions. A detailed investigation of aluminum agglomeration and other surface processes as influenced by pressure and formulation variables such as aluminum particle size and loading, ammonium perchlorate size distribution, binder type, and burning rate catalyst would be of great help in understanding how these variables influence the ballistic properties of the propellant. The photographic technique can also be used to measure the burning rate of aluminum particles, which has so far been determined only in burner or other simulated experiments, in actual solid propellant combustion gases.

REFERENCES

1. Compilation of Rocket Spin Data. NASA CR 66641 (Contract No. NAS1-6833), Emerson Electric and Space Division, July 1968.
2. Investigation of Internal Ballistic Effects in Spinning Solid Propellant Motors. Final Report UTC 2281-FR (Contract No. N00017-67-C-2429), United Technology Center, October 1968.
3. Investigation of Performance Losses and Ballistics Effects in Solid Propellant Rockets. Final Report UTC 2197-FR (Contract No. NOw 66-0444-c), United Technology Center, April 1967.
4. Investigation of Particle Growth and Ballistic Effects on Solid Propellant Rockets. Final Report UTC 2128-FR (Contract No. NOw 65-0222-f), United Technology Center, June 1966.
5. Northam, G. B.; and Lucy, M. H.: On the Effects of Acceleration Upon Solid Rocket Performance. Presented at the Third ICRPG/AIAA Solid Propulsion Conference, Atlantic City, New Jersey, 4 through 6 June 1968.
6. Northam, G. B.: An Experimental Investigation of the Effects of Acceleration on the Combustion Characteristics of an Aluminized Composite Solid Propellant. M.S. Thesis, Virginia Polytechnic Institute, June 1965.
7. Sturm, E. J.; and Reichenbach, R. E.: An Experimental Study of the Burning Rates of Aluminized Composite Propellants in Acceleration Fields. AIAA Paper No. 68-529 presented at the Third ICRPG/AIAA Solid Propellant Propulsion Conference, Atlantic City, New Jersey, 4 through 6 June 1968.
8. Anderson, J. B.; and Reichenbach, R. E.: An Investigation of the Effect of Accereration on the Burning Rate of Composite Propellants. Report No. NPS-57-RV7071A, United States Naval Postgraduate School, 28 July 1967.
9. Northam, G. B.: Acceleration-Induced Transient Burning-Rate Augmentation of an Aluminized Solid Rocket Propellant. Ph.D. Thesis, Virginia Polytechnic Institute, June 1969.
10. Crump, J. E.: Aluminum Combustion in Composite Propellants. Presented at the Second ICRPG Combustion Conference, 1 through 5 November 1965.
11. Willoughby, P. G.; Crowe, C. T.; and Baker, K. L.: A Photographic and Analytic Study of Composite Propellant Combustion in an Acceleration Field. AIAA Paper No. 69-173 presented at the Seventh Aerospace Sciences Meeting, New York, N.Y., 20 through 22 January 1969.
12. Dunlap, R.; and Hermsen, R. W.: Impingement of Aluminum and Aluminum Oxide Particles on Aft Closures of Titan III-C, Titan IIIM and Subscale IIIM Motors. Technical Memorandum TM-33-69-U2, United Technology Center, May 1969.
13. Glick, R. L.: An Analytical Study of the Effects of Radial Acceleration Upon the Combustion Mechanism of Solid Propellant. NASA Report No. 66218 (Contract No. NAS 7-406), Thiokol Chemical Corporation, December 1966.

APPENDIX A

PROPELLANT FORMULATION, BALLISTIC CHARACTERISTICS, AND PHYSICAL PROPERTIES

This appendix presents the propellant formulations used, their motor ballistic characteristics, and physical properties. Additional ballistic information is given which was obtained on the UTC propellants burning in the photographic combustion bomb.

The burning rate versus pressure characteristics of the propellant formulations listed below are shown in figure A-1. The quoted mass median particle diameters, d_m, of the individual constituents represent the specification value of this average particle size and are only nominal.

Propellant I $\quad \dot{r} = 0.25 \left[\frac{P_c}{1{,}000}\right]^{0.21}$

16% PBAN Binder (UTC)

68% AP: 65% 400μ; 35% 8μ

16% Al: 46μ (Valley Metallurgical H-322)

Propellant II $\quad \dot{r} = 0.35 \left[\frac{P_c}{1{,}000}\right]^{0.20}$

16% PBAN Binder (UTC)

68% AP: 40% 190μ; 60% 8μ

16% Al: 46μ (Valley Metallurgical H-322)

Propellant III* $\quad \dot{r} = 0.34 \left[\frac{P_c}{1{,}000}\right]^{0.28}$

16% PBAN Binder (UTC)

68% AP: 65% 400μ; 35% 8μ

16% Al: 8μ (Valley Metallurgical H-5)

* Ballistic data for propellants I, II, and III were obtained with micromotors (32 or 145 grams of propellant). Previous 4-lb ballistic firings correlated well with the micromotor data for propellants I and II; however, 4-lb ballistic firings of propellant III indicate that $\dot{r} = 0.25$ in./sec at 750 psi, significantly lower than the micromotor data.

Propellant IV $\dot{r} = 0.13 \left[\frac{P_c}{1{,}000}\right]^{0.06}$

25% Polyurethane (BFG)
57% AP 200μ
18% Al 26μ (Alcoa 123)

Propellant V $\dot{r} = 0.56 \left[\frac{P_c}{1{,}000}\right]^{0.42}$

16% CTPB Binder

68% AP 70% 200μ
30% 20μ

16% Mg/Al Alloy

Propellant VI $\dot{r} = 0.37 \left[\frac{P_c}{1{,}000}\right]^{0.25}$

14% PBAA Binder (Thiokol AA)

70% AP 70% 190μ
30% 20μ

16% Al 7μ (Reynolds 400)

Typical physical properties of propellants I, II, and III are:

Maximum Stress (psi)	Strain at Maximum Stress (in./in.)	Temperature (^{o}F)
845	.13	-40
410	.27	0
144	.51	75
43	.42	160

with $\pi_K = 0.15 - 0.2\%$ in./sec/^{o}F, and $\rho = 0.063$ lb/in.^{3}

In addition to the above data, figure A-2 presents data for propellants I, II, and III obtained in the photographic combustion bomb. It may be noted that the data lie below the motor data and exhibit a higher burning rate exponent. The reduced burning rates must be a result of heat losses augmented by the flowing nitrogen purge gas. A detailed understanding of the relative contributions of radiative and

convective heat transfer to the burning surface as a function of pressure would be required to explain the magnitude of the reduced burning rate and the change in burning rate exponent, but it is evident that the combustion characteristics of the propellants are altered when they are burned in the photographic combustion bomb. However, in view of the fine correlation between the photographic observations and those made on slab burners and subscale motor firings, the mechanism apparent from the photographic studies appears to have general validity.

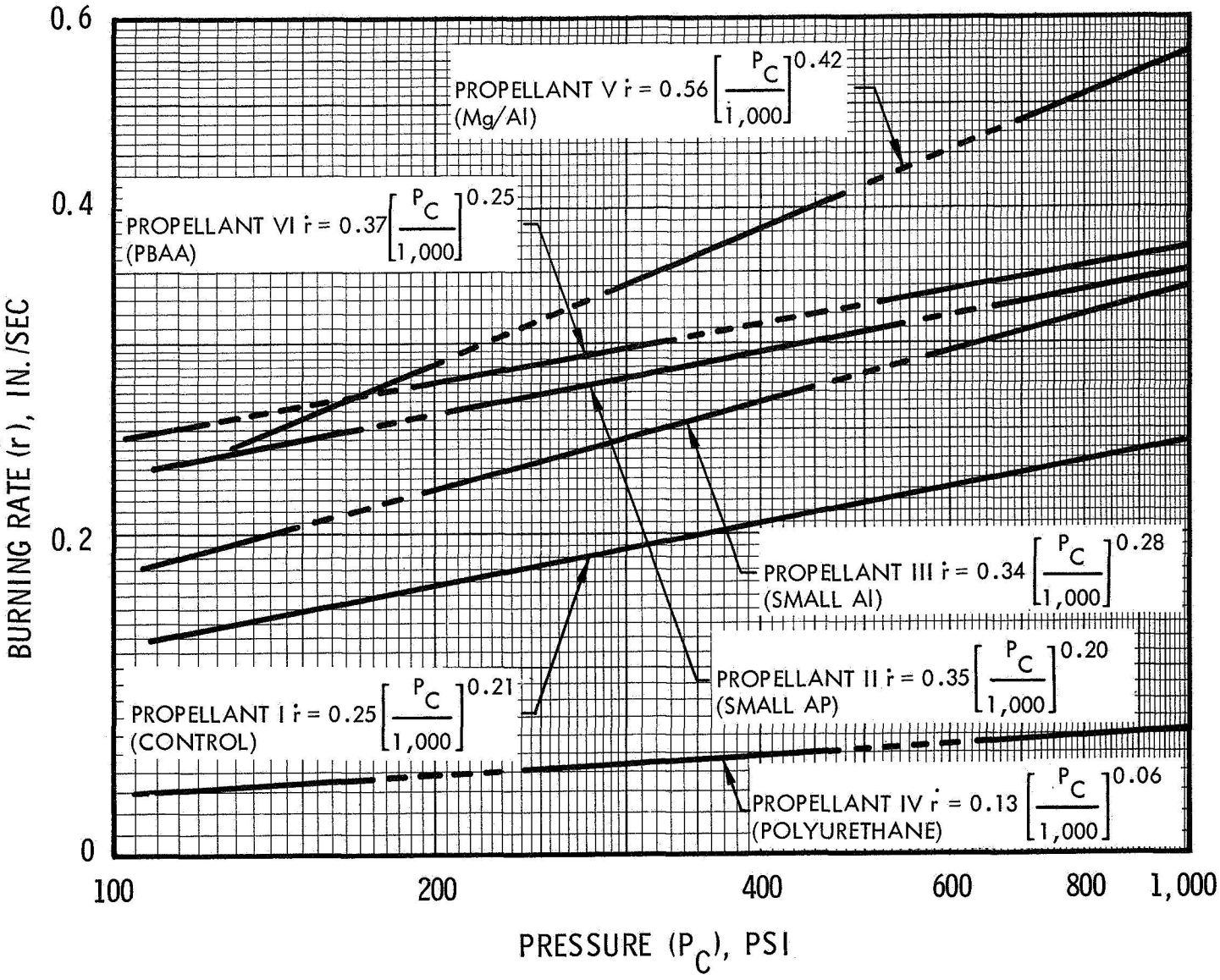

Figure A-1. Burning Rate vs Chamber Pressure

91503

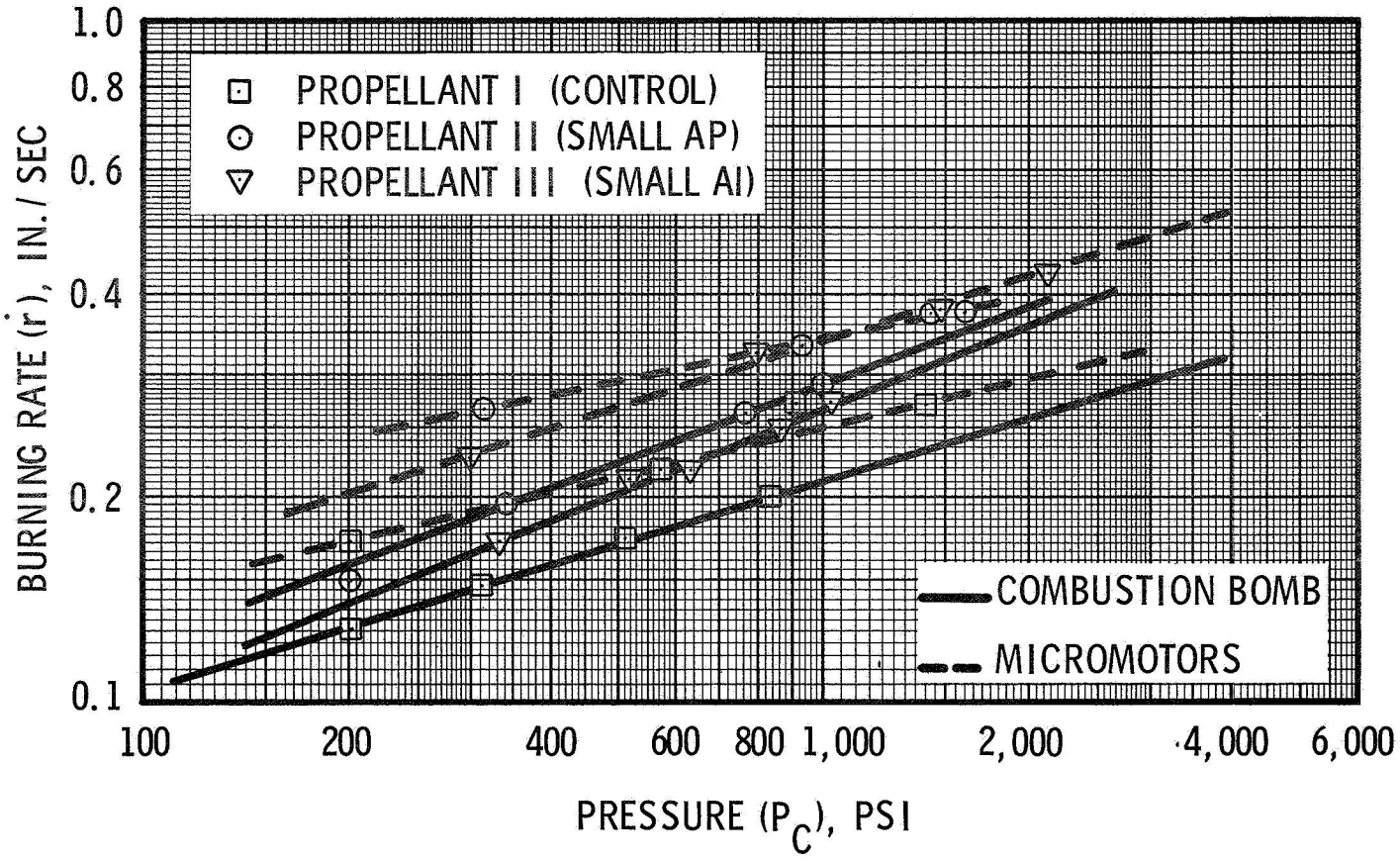

Figure A-2. Burning Rate vs Chamber Pressure for Combustion in Micromotors and Photographic Combustion Bomb

91504